

---

# PLANNING TO FAIRLY ALLOCATE: PROBABILISTIC FAIRNESS IN THE RESTLESS BANDIT SETTING

---

Christine Herlihy\*

Aviva Prins\*

Aravind Srinivasan

John Dickerson

Department of Computer Science, University of Maryland, College Park, MD, USA  
{cherlihy, aviva, srin, john}@cs.umd.edu

## ABSTRACT

Restless and collapsing bandits are commonly used to model constrained resource allocation in settings featuring arms with action-dependent transition probabilities, such as allocating health interventions among patients [Whittle, 1988; Mate et al., 2020]. However, state-of-the-art Whittle-index-based approaches to this planning problem either do not consider fairness among arms, or incentivize fairness without guaranteeing it [Mate et al., 2021]. Additionally, their optimality guarantees only apply when arms are indexable and threshold-optimal. We demonstrate that the incorporation of hard fairness constraints necessitates the coupling of arms, which undermines the tractability, and by extension, indexability of the problem. We then introduce PROBFair, a probabilistically fair stationary policy that maximizes total expected reward and satisfies the budget constraint, while ensuring a strictly positive lower bound on the probability of being pulled at each timestep. We evaluate our algorithm on a real-world application, where interventions support continuous positive airway pressure (CPAP) therapy adherence among obstructive sleep apnea (OSA) patients, as well as simulations on a broader class of synthetic transition matrices.

## 1 Introduction

Restless multi-arm bandits (RMABs) are used to model resource-constrained sequential decision-making, in which the states of the arms under consideration evolve over time in an action-dependent Markovian way. Many such problems exist in the healthcare setting, where budget-limited interventions must be allocated to maximize well-being across a patient cohort. For example, RMABs have been proposed for prioritizing patients to receive hepatitis C treatment in U.S. prisons [Ayer et al., 2019], and tuberculosis-medication adherence-promoting support in India [Mate et al., 2020]. When designing such clinical decision support programs, acceptability is improved when domain expertise and fairness considerations are incorporated [Rajkomar et al., 2018; Kelly et al., 2019]. Indeed, when a pull is associated with an increased probability of a favorable state transition, domain experts tasked with executing the policy may consider a zero-valued lower bound to be ethically unacceptable, and deviate in favor of sub-optimal but more equitable round-robin approaches [De-Arteaga et al., 2020].

Current state-of-the-art solutions to these RMAB problems rely on the indexing work introduced by Whittle [1988]. While the Whittle index allows us to solve an otherwise intractable problem by decoupling arms, existing approaches focus on maximizing total expected reward over all arms and timesteps, and fail to provide any guarantees about how pulls will be distributed [Prins et al., 2020].

We study the introduction of Rawlsian constraints on the distribution of actions in this conventionally utilitarian setting to ensure that utility is maximized and each arm is guaranteed to derive some benefit from participation. We specifically consider the introduction of a *probabilistic fairness* constraint that encodes the requirement that an arm will be pulled with some strictly positive probability at each timestep, and develop a stationary-policy-based algorithm that enforces this constraint. We evaluate our results on both a realistic dataset derived from continuous positive airway pressure (CPAP) therapy treatment adherence behavior for patients diagnosed with obstructive sleep apnea (OSA), and simulated datasets representing a wider range of cohort composition scenarios (Section 6). We find that our algorithm maintains utility while providing fairness guarantees.

---

\*Denotes equal contribution

## 2 Restless Multi-Arm Bandits

### 2.1 Model Components

We consider the restless multi-arm bandit (RMAB) setting, which can be characterized by a 4-tuple,  $(N, T, k, R)$ , with  $N \in \mathbb{Z}^+$  representing the number of arms, each of which is associated with a Markov decision process (MDP),  $T \in \mathbb{Z}^+$  representing the number of timesteps,  $k \ll N \in \mathbb{Z}^+$  representing the per-timestep budget, and  $R(\cdot)$  representing the cumulative reward function [Whittle, 1988]. At each timestep  $t \in T$ , the agent can select at most  $k$  out of  $N$  restless arms. The agent’s goal is to find a policy  $\pi^*$  that maximizes total expected reward  $\mathbb{E}_\pi[R(\cdot)]$ :  $\pi^* := \arg \max_\pi \mathbb{E}_\pi[R(\cdot)]$ .

*Restlessness* refers to the fact that the state of each arm can evolve over time, in accordance with its associated MDP. Each arm’s MDP is characterized by a 4-tuple,  $(\mathcal{S}, \mathcal{A}, P, r)$ , where  $\mathcal{S}$  represents the state space,  $\mathcal{A}$  represents the action space,  $P_{s,s'}^{a \in \mathcal{A}}$  represents the transition matrix associated with each action, and  $r(\cdot)$  represents a local reward function that maps action-driven state transitions  $(s, a, s')$  at each timestep to rewards  $\in \mathbb{R}$  (see Table 1 in Appendix A.1).

We specifically consider a discrete two-state system,  $\mathcal{S} := \{0, 1\}$ , where 1 (0) represents being in the ‘good’ (‘bad’) state and two action options,  $\mathcal{A} := \{0, 1\}$ , where 1 represents the decision to act (pull) arm  $i \in [N]$  at time  $t$ , else 0 represents the choice to be passive (not pull). Each arm  $i$  is characterized by a set of action-indexed transition matrices, which we assume to be both (a) static and (b) known by the agent at planning time. We note that these assumptions are likely to be violated in practice; however, they provide a useful modeling foundation, and can be modified to incorporate additional uncertainty, such as the requirement that transition matrices must be learned [Jung and Tewari, 2019]. Indeed, clinical researchers often use longitudinal data to construct risk-adjusted transition matrices that encode cohort-specific transition probabilities that can be used to inform patient-level decision-making [Steimle and Denton, 2017].

Per Mate et al. [2020], we assume strictly positive transition matrix entries, and impose four *structural constraints*: (a)  $P_{0,1}^0 < P_{1,1}^0$ ; (b)  $P_{0,1}^1 < P_{1,1}^1$ ; (c)  $P_{0,1}^0 < P_{0,1}^1$ ; (d)  $P_{1,1}^0 < P_{1,1}^1$ . These constraints are application-motivated, and imply that arms are more likely to remain in a ‘good’ state than change state from a bad state to a good one, and that a pull (intervention) is helpful when received.

In the general RMAB setting outlined above, each arm’s state  $s_t^i$  is observable. Mate et al. [2020] introduce the partially-observable variant *Collapsing Bandits*. If  $a_t^i = 1$ , arm  $i$  is pulled at time  $t$  and its latent state  $s_t^i \in \mathcal{S}$  is learned. Otherwise, the arms’ state is approximated with the probabilistic *belief* that it is in state 1,  $b_t^i \in [0, 1]$ . Such partial observability captures the uncertainty regarding patient status and treatment efficacy associated with outpatient or remotely-administered interventions.

The global reward function,  $\mathbb{E}_\pi[R(\cdot)]$ , that the agent seeks to maximize is a function of each arm’s local reward function,  $r$ :  $\mathbb{E}_\pi[R(r(s))]$ . Two types of reward  $R(\cdot)$  have been considered in the literature: discounted and average. Discounted reward is defined as  $\bar{R}(\cdot) := \sum_{i \in [N]} \sum_{t \in [T]} \beta^t r(s_t^i)$  for some discount rate  $\beta \in [0, 1]$ . The average reward,  $\bar{R}(\cdot) := \frac{1}{T} \sum_{i \in [N]} \sum_{t \in [T]} r(s_t^i)$ , is the undiscounted sum of rewards normalized by time.

### 2.2 The Whittle Index

Pre-computing the optimal policy for a given set of restless or collapsing arms is PSPACE-hard in the general case [Papadimitriou and Tsitsiklis, 1994]. However, as established by Whittle [1988] and formalized by Weber and Weiss [1990], if the set of arms associated with a problem instance are *indexable*, it is possible to decouple the arms and efficiently solve the problem using an asymptotically optimal heuristic index policy.

The mechanics of this approach are as follows: at each timestep  $t \in T$ , the value of a pull, in terms of both immediate and expected discounted future reward, is computed for each decoupled arm,  $i \in [N]$ . This value computation step relies on the notion of a subsidy,  $m$ , which can be thought of as the opportunity cost of passivity. Formally, the Whittle index is the subsidy required to make the agent indifferent between *pulling* and *not pulling* arm  $i$  at time  $t$ :

$$W(b_t^i) = \inf_m \{m \mid V_m(b_t^i, a_t^i = 0) \geq V_m(b_t^i, a_t^i = 1)\} \quad (1)$$

where the value function  $V_m(b)$  represents the maximum expected discounted reward under passive subsidy  $m$  and discount rate  $\beta$  for collapsing arm  $i$  with belief state  $b_t^i \in [0, 1]$  at time  $t$  (note that for restless arms,  $b_t^i = s_t^i \in \{0, 1\}$ ):

$$V_m(b_t^i) = \max \begin{cases} m + r(b_t^i) + \beta V_m(b_{t+1}^i) & \text{passive } (a_t^i = 0) \\ r(b_t^i) + \beta [b_t^i V_m(P_{1,1}^1) + (1 - b_t^i) V_m(P_{0,1}^1)] & \text{active } (a_t^i = 1) \end{cases} \quad (2)$$

Once the Whittle index has been computed for each arm, the agent sorts and the  $k$  arms with the greatest index values receive a pull at time  $t$ , while the remaining  $N - k$  arms are passive. Weber and Weiss [1990] give sufficient conditions for indexability:

**Definition 1** (*Indexability*) An arm is indexable if the set of beliefs for which it is optimal to be passive for a given value of  $m$ ,  $\mathcal{B}^*(m) = \{b \mid \forall \pi \in \Pi_m^*, \pi(b) = 0\}$ , monotonically increases from  $\emptyset$  to the entire belief space as  $m$  increases from  $-\infty$  to  $+\infty$ . An RMAB system is indexable if every arm is indexable.

Indexability is often difficult to establish, and computing the Whittle index can be complex [Liu and Zhao, 2010]. Prevailing approaches for proving indexability rely on proving the optimality of a *threshold policy* for a subset of transition matrices [Niño-Mora, 2020]. A *forward* threshold policy pulls an arm when its state is at or above a given threshold, and makes an arm passive otherwise; the converse is true for a *reverse* threshold optimal policy. Mate et al. [2020] give such conditions for this RMAB setting, when  $r(b) = b$ , and provide the THRESHOLD WHITTLE that is asymptotically optimal for forward threshold arms. Mate et al. [2021] expand on this work for any non-decreasing  $r(b)$  and present the RISK-AWARE WHITTLE algorithm. As far as we are aware, no algorithm exists for reverse threshold optimal arms.

### 3 Algorithmic Distributive Fairness

Multi-arm bandit optimization problems are canonically framed from the perspective of the decision-maker; interest in individual and group fairness in this setting is a relatively recent phenomenon [Joseph et al., 2016]. To the extent that fairness among arms has been considered in the literature, existing approaches either do not consider restless arms [Chen et al., 2020; Li et al., 2019], or redistribute pulls without providing arm-level guarantees Mate et al. [2021].

#### 3.1 Individual Welfare Under Whittle-based Policies

When a Whittle index-based policy is used to select  $k$  arms at each timestep in the RMAB setting, existing theory does not offer any guarantees about how the resulting sequence of  $T \times k$  pulls will be distributed over arms, or the probability with which a given arm will be pulled at any particular timestep. Prins et al. [2020] demonstrate Whittle-based policies tend to allocate all resources to a small number of arms, neglecting most of the population. We present similar findings in Appendix A.5.1.

This zero-valued lower bound on the number of pulls that any given arm can receive is consistent with a *utilitarian* approach to distributive justice, in which the decision-maker seeks to allocate resources so as to maximize total expected utility [Bentham, 1781; Marseille and Kahn, 2019]. However, this may be incompatible with competing pragmatic and ethical desiderata, including *egalitarian* and *prioritarian* notions of distributive fairness, in which the decision-maker allocates seeks to allocate resources equally among arms (e.g., round-robin) or prioritize arms considered to be worst off under the status quo, for some quantifiable notion of *worst off* that induces a partial ordering over arms [Rawls, 1971; Scheunemann and White, 2011].

For our purposes, we consider the *worst off* arms to be those who would be deprived of algorithmic attention (e.g., not receive any pulls), or, from a probabilistic perspective, would have a zero-valued lower bound on the probability of receiving a pull at any given timestep, under THRESHOLD WHITTLE. In particular, we want to ensure that: (1) practitioners tasked with implementing a policy find it to be ethically acceptable, so as to minimize the loss of reward associated with uncoordinated deviation en masse [Dietvorst et al., 2015]; and (2) arms find participation in the intervention program to be rational.

#### 3.2 Fairness-motivated Constraints on Actions

We consider three types of fairness constraints enforced at planning time: (a) hard integer periodicity, (b) probabilistic fairness, and (c) minimum selection fraction [Li et al., 2019].

The **hard integer periodicity constraint** allows a decision-maker to guarantee that arm  $i$  is pulled at least once within each period of  $\nu$  days. We define this constraint as a function  $g$ , over the vector of actions,  $\vec{a}^i$  associated with arm  $i$ , and user-defined interval length  $\nu \in [1, T]$ :

$$g(\vec{a}^i) = \sum_{t=j\nu+1}^{(j+1)\nu} a_t^i \geq 1 \quad \forall j \in \left\{0, 1, 2, \dots, \left\lceil \frac{T}{\nu} \right\rceil\right\} \quad \text{and } i \in \{1, 2, \dots, N\} \quad (3)$$

The **probabilistic constraint** encodes the requirement that arm  $i$  will be pulled with some probability  $p_i$  in a given range  $[\ell, u]$  at each timestep  $t \in T$ , where  $\ell \in (0, \frac{k}{N}]$  and  $u \in [\frac{k}{N}, 1]$ .

Finally, Li et al. [2019] define a **minimum selection fraction constraint**, which strictly requires the agent to pull arm  $i$  at least some minimum fraction,  $\psi \in (0, 1)$ , of the total number of timesteps, but is agnostic to how these pulls are

distributed over time. We define this constraint,  $g'$ , as a function over the vector of actions,  $\vec{a}^i$  associated with arm  $i$ , and user-supplied  $\psi$ :

$$g'(\vec{a}^i) = \frac{1}{T} \sum_{t=1}^T a_t^i \geq \psi \quad \forall i \in \{1, 2, \dots, N\} \quad (4)$$

However, the optimal policy under this constraint is to dismiss constraint-motivated pulls to the beginning or end of the task, and follow the unfair optimal policy for intermediate timesteps. As our motivating applications include programs with large horizons  $T$  and the sequential pattern of adherence over time is clinically meaningful, this fairness constraint is not well-suited for our problem, so discussion of it is relegated to Appendix A.5.2.

## 4 Hard Fairness Constraint Enforcement and Tractability

### 4.1 Hard Fairness Guarantees in the Planning Setting Require Coupled Arms

The efficiency of Whittle index-based policies stems from our ability to decouple arms when we are only concerned with maximizing total expected reward [Whittle, 1988; Weber and Weiss, 1990]. However, enforcing the hard integer periodicity and minimum selection fraction constraints introduced in Section 3.2 in the planning setting requires time-stamped record keeping. It is no longer sufficient to compute each arm’s infimum subsidy in isolation and order the resulting set of values. Instead, for an optimal index policy to be efficiently computable, it must be possible to modify the value function so as to ensure that the infimum subsidy each arm would require in the absence of fairness constraints is minimally perturbed via augmentation or “donation”, so as to maximize total expected reward while ensuring its own fairness constraint satisfaction or the constraint satisfaction of other arms, respectively, *without* requiring input from other arms.

Plausible modifications include altering the conditions under which an arm receives the subsidy associated with passivity,  $m$ , or introducing a modified reward function,  $r'(b)$  that is capable of accounting for an arm’s fairness constraint satisfaction status in addition to its state at time  $t$ . For example, we might use an indicator function to “turn off” the subsidy until arm  $i$  has been pulled at least once within the interval in question, or increase reward as an arm’s time-since-pulled value approaches the interval cut-off, so as to incentivize a constraint-satisfying pull. When these modifications are viewed from the perspective of a single arm, they *appear* to have the desired effect: if no subsidy is received, it will be optimal to pull for all belief states; similarly, for a fixed  $m$ , as reward increases it will be optimal to pull for an increasingly large subset of the belief state space.

Recall, however, that structural constraints ensure that when an arm is considered in isolation, the optimal action will *always* be to pull. Whether or not arm  $i$  is *actually* pulled at time  $t$  depends on how the infimum subsidy,  $m$ , it requires to accept passivity at time  $t$  compares to the infimum subsidies required by other arms. Thus, any modification intended to *guarantee* hard fairness constraint satisfaction must be able to alter the ordering *among* arms, such that any arm  $i$  which would otherwise have a subsidy with rank  $> k$  when sorted descending will now be in the top- $k$  arms. Even if we were able to construct such a modification for a single arm without requiring system state, if *every* arm had this same capability, then a new challenge would arise: we would be unable to distinguish among arms, and arbitrary tie-breaking could again jeopardize fairness constraint satisfaction. If it is not possible to decouple arms, then we must consider them in tandem. Papadimitriou and Tsitsiklis [1994] prove that the RMAB problem is PSPACE-complete even when transition rules are action-dependent but deterministic, via reduction from the halting problem.

### 4.2 Challenges of an Integer Programming Solution Approach

Since we are not able to guarantee hard fairness constraint satisfaction with decoupled arms, we must look beyond Whittle to identify efficient algorithmic alternatives. A motivating question we consider in this context is: what is the maximum total reward we can expect to achieve in expectation, given both budget *and* hard fairness constraint satisfaction? To build intuition, we formulate this problem as an integer program (IP), where each decision variable  $x_{i,a,t} \in \{0, 1\}$  represents whether or not we take action  $a$  for arm  $i$  at time  $t$ , and each objective function coefficient  $c_{i,a,t}$  represents the expected reward associated with each arm-action-timestep combination—that is,  $\mathbb{E}_s[p(s_{t+1} = 1 | x_{i,a,t}, s_t)]$ .

It is straightforward to encode the binary nature of each decision variable, along with budget and either of the hard equity constraints in space polynomial in the inputs of order  $O(N^2 T^2 |\mathcal{A}|)$ . Additionally, we prove in Appendix A.2.2 that any feasible problem instance will yield a totally unimodular constraint matrix, which ensures that the linear program (LP) relaxation of our IP will yield an integral solution. However, one insurmountable challenge remains: in the planning setting, we do not know which state arm  $i$  will be in at time  $t$  or which actions we will have taken in previous timesteps. Thus, exact computation of the expected reward terms contained within the polynomial-length coefficient vector,  $\vec{c}$ , requires us to enumerate  $N$  game trees, each of order  $O(|\mathcal{S}| |\mathcal{A}|^T)$ .

## 5 Probabilistically Fair Stationary Policy

### 5.1 Overview and Motivation

The tractability concerns associated with the exact computation of the objective-function coefficients outlined in Section 4 motivate us to consider efficient alternative approaches that avoid exponential dependency on  $T$ . One such approach is a *probabilistically fair stationary policy*  $\pi_{PF}$  that maps each arm  $i$  to a probability of being pulled,  $p_i \in [\ell, u]$ , such that  $\sum_i p_i \leq k$  and  $0 < \ell \leq p_i \leq u \forall i \in [N]$ . Here,  $0 < \ell \leq u \leq 1$  are user-defined fairness parameters such that  $\ell \leq \frac{k}{N} \leq u$ . See Section 5.3 for how to sample from such a distribution at every timestep *independently*, such that at most  $k$  arms are pulled in each timestep with probability one. The  $p_i$ 's are variables constrained as above; we will formulate our objective and solve for the  $p_i$ 's to maximize this objective in Section 5.2. Note that fairness is explicitly expressed in the constraints. Furthermore, we also have stronger forms of fairness: e.g., if  $u \leq 2\ell$ , then we know that with high probability, any arm will be pulled at most, say, 2.1 times as often as any other arm, over any given sufficiently-long sequence of timesteps. Thus, we argue that our sort of formulation guarantees probabilistic fairness that can be solved for—as in Section 5.2—with *no* dependence on  $T$ . We call our algorithm PROBFair and compare it against the LP introduced in Section 4.2 in Appendix A.5.2.

Fix an arm  $i$ . Stationarity in this context refers to the distribution over the state space,  $\mathcal{S}$ , induced by the policy which pulls arm  $i$  with probability  $p_i$  at each timestep, independently of past realized actions. Regardless of the arm's initial state, the repeated application of this policy will result in convergence to a stationary distribution, in which the arm is in the adherent state (e.g., state 1) with probability  $x = x_i \in [\ell, u]$  and the non-adherent state (e.g., state 0) with probability  $1 - x \in [0, 1]$ . By definition,  $x$  will satisfy the equation:

$$x [(1 - p_i)P_{1,1}^0 + p_iP_{1,1}^1] + (1 - x)[(1 - p_i)P_{0,1}^0 + p_iP_{0,1}^1] = x \quad (5)$$

Thus,  $x = x_i = f_i(p_i)$ , where:

$$f_i(p_i) = \frac{(1 - p_i)P_{0,1}^0 + p_iP_{0,1}^1}{1 - (1 - p_i)P_{1,1}^0 - p_iP_{1,1}^1 + (1 - p_i)P_{0,1}^0 + p_iP_{0,1}^1} \quad (6)$$

For convenience, let:

$$c_1 = P_{0,1}^0; \quad c_2 = P_{0,1}^1 - P_{0,1}^0; \quad c_3 = 1 - P_{1,1}^0 + P_{0,1}^0; \quad c_4 = P_{1,1}^0 - P_{1,1}^1 - P_{0,1}^0 + P_{0,1}^1. \quad (7)$$

Then,  $f_i(p_i) = \frac{c_1 + c_2 p_i}{c_3 + c_4 p_i}$ . We observe that  $\forall i \in [N]$ ,  $f_i(p_i)$  is a valid probability since the term  $1 - (1 - p_i)P_{1,1}^0 - p_iP_{1,1}^1$  in the denominator is at least  $1 - (1 - p_i) - p_i = 0$  for all  $p_i \in [0, 1]$ . We begin by considering the shape of  $f_i(p_i)$ . There are three cases:

**Case 1**  $c_4 = 0$ . Here,  $f_i(p_i)$  is *linear* and hence, e.g., *concave*.

**Case 2**  $c_4 \neq 0; c_2 = 0$ . Here,  $f_i''(p_i) = \frac{2c_1 c_4^2}{(c_3 + c_4 p_i)^3} \geq 0$ , so  $f_i(p_i)$  is *linear* (hence *concave*) if  $c_1 = 0$  or *strictly convex* (if  $c_1 > 0$ ) in the domain  $p_i \in [0, 1]$ .

**Case 3**  $c_4 \neq 0; c_2 \neq 0$ . Here,

$$f_i(p_i) = \frac{\frac{c_2}{c_4} \left( \frac{c_1 c_4}{c_2} + c_4 p_i \right)}{c_3 + c_4 p_i} = \frac{c_2}{c_4} + \frac{\left( c_1 - \frac{c_2 c_3}{c_4} \right)}{c_3 + c_4 p_i}. \quad (8)$$

Thus,  $f_i''(p_i) = \frac{2c_4^2 \left( c_1 - \frac{c_2 c_3}{c_4} \right)}{(c_3 + c_4 p_i)^3}$ , whose sign is the same as the sign of  $d = c_1 - \frac{c_2 c_3}{c_4}$ . It follows that  $f_i(p_i)$  is *strictly convex* for  $p_i \in [0, 1]$  if  $c_1 > \frac{c_2 c_3}{c_4}$ , and *concave* for  $p_i \in [0, 1]$  otherwise.

The structural constraints introduced in Section 2.1 ensure that  $f_i(p_i)$  is monotonically non-decreasing in  $p_i$  over the interval  $(0,1)$  for every arm  $i \in [N]$ , as illustrated below:

$$f_i'(p_i) = \frac{c_2 c_3 - c_1 c_4}{(c_3 + c_4 p_i)^2} \quad c_2 c_3 - c_1 c_4 \geq 0 \rightarrow f_i'(p_i) \geq 0 \quad (9)$$

$$c_2 c_3 - c_1 c_4 = (P_{0,1}^1 - P_{0,1}^0)(1 - P_{1,1}^0 + P_{0,1}^0) - P_{0,1}^0(P_{1,1}^0 - P_{1,1}^1 - P_{0,1}^0 + P_{0,1}^1) \quad (10)$$

$$(P_{0,1}^1 - P_{0,1}^0)(1 - P_{1,1}^0 + P_{0,1}^0) \geq P_{0,1}^0(P_{1,1}^0 - P_{1,1}^1 - P_{0,1}^0 + P_{0,1}^1) \quad (11)$$

$$(1 - P_{1,1}^0)P_{0,1}^1 \geq (1 - P_{1,1}^1)P_{0,1}^0 \quad \text{per structural constraints, } P_{1,1}^0 < P_{1,1}^1; P_{0,1}^1 > P_{0,1}^0 \quad (12)$$

## 5.2 Computing the $p_i$ 's: Optimization Formulation and Algorithm

We frame the task of finding a reward-maximizing, probabilistically fair stationary policy as a mathematical program, in which we seek to maximize  $\sum_i f_i(p_i)$  subject to  $\sum_i p_i \leq k$  and  $p_i \in [\ell, u] \forall i \in [N]$ . Note that the maximization objective is the long-term expected number of times we pull arms (we ignore the initial short “burn in” period as each arm approaches stationarity: these periods are especially short as each arm is just a two-state Markov chain). We show how to construct the  $p_i$ 's efficiently in order to approximate this objective to within a multiplicative  $(1 - \epsilon)$  efficiently, for any given constant  $\epsilon > 0$ . The discussion in Section 5.1 shows that we can view our problem as follows: (i) each  $f_i$  is non-decreasing in our domain, and hence our constraint “ $\sum_i p_i \leq k$ ” becomes

$$\sum_i p_i = k \text{ and } \forall i, p_i \in [\ell, u]; \quad (13)$$

(ii) each  $f_i(p_i)$  is given to be either concave in all of  $p_i \in [0, 1]$ , or strictly convex in all of  $p_i \in [0, 1]$ . This mixture makes our problem challenging, but still solvable as we show next. Let  $A = \{i : f_i \text{ is concave}\}$  and  $B = [N] - A = \{i : f_i \text{ is strictly convex}\}$ . Recall our basic constraint (13). By a one-dimensional grid search, we search over all  $z \in [0, k]$  such that in an optimal solution,  $\sum_{i \in A} p_i = z$ . While of course almost all of the considered  $z$ 's will be incorrect and will thus lead to suboptimal solutions, one of them will be correct (to within the approximation error of the grid search). Thus, if we take the highest objective-function value obtained over all the  $z$ 's, we will obtain a near-optimal solution; thus we may assume from here on that we have obtained the correct  $z$ . Given such a  $z$ , our problem decomposes into two *independent* subproblems:

**(P1)** maximize  $\sum_{i \in A} f_i(p_i)$  subject to:  $p_i \in [\ell, u]$  for all  $i \in A$ , and  $\sum_{i \in A} p_i = z$ ; and

**(P2)** maximize  $\sum_{i \in B} f_i(p_i)$  subject to:  $p_i \in [\ell, u]$  for all  $i \in B$ , and  $\sum_{i \in B} p_i = k - z$ .

(P1) is a concave-maximization problem, solvable efficiently by gradient descent; we thus need only focus on (P2). For (P2), we first claim a key **structural result**: (P2) has an optimal solution in which  $p_i \in (\ell, u)$  for at most one  $i \in B$ , which we prove in Appendix A.3.1. Given this structure, an optimal solution  $\vec{p}$  to (P2) either has: **(i)** an integer  $\gamma \in [0, |B|]$  such that  $\gamma\ell + (|B| - \gamma)u = k - z$ , and with exactly  $\gamma$ -many  $i \in B$  having  $p_i = \ell$ , and with the other  $(|B| - \gamma)$ -many  $i' \in B$  having  $p_{i'} = u$ , or **(ii)** an integer  $\gamma \in [0, |B| - 1]$  and a  $z' \in (\ell, u)$  such that  $\gamma\ell + (|B| - 1 - \gamma)u + z' = k - z$ , and with exactly  $\gamma$ -many  $i \in B$  having  $p_i = \ell$ ,  $(|B| - 1 - \gamma)$ -many other  $i' \in B$  having  $p_{i'} = u$ , and one other  $j \in B$  having  $p_j = z'$ . It is easy to distinguish these two cases and to find  $\gamma$  (and  $z'$  in case (ii)); we mainly consider case (i) and then sketch the proof for case (ii).

In Case (i), we are given  $\gamma$ , and want to find the optimal subset  $B' \subseteq B$  of cardinality  $\gamma$  such that  $p_i = \ell$  for all  $i \in B'$  and  $p_{i'} = u$  for all  $i' \in (B - B')$ , so that  $\sum_{i \in B} f_i(p_i)$  is maximized. Recall that each  $f_i$  is non-decreasing: take  $\gamma$  distinct indices  $i \in B$  with the smallest values of  $(f_i(u) - f_i(\ell))$  and make these the members of  $B'$ . In Case (ii), we iterate over each  $j \in B$  and then find  $B'$  by an algorithm essentially the same as in Case (i), which incurs a multiplicative factor of  $|B|$ —due to the search over  $j$ —as compared to the run-time for Case (i). The rest of the proof is the same as Case (i).

## 5.3 Sampling Approach

For problem instances with feasible solutions, the mathematical program outlined in Section 5.2 returns a real-valued mapping from arms to probability values,  $\pi_{PF} : i \mapsto p_i \in [\ell, u]$ . By virtue of the fact that  $\ell > 0$ , this policy guarantees probabilistic fairness constraint satisfaction for all arms. We leverage a linear-time algorithm introduced by Srinivasan [2001] and detailed in Appendix A.3.2 to sample from  $\pi_{PF}$  at each timestep, such that the following properties hold: (1) with probability one, we satisfy the budget constraint by pulling exactly  $k$  arms; and (2) for any given arm  $i$ , it is pulled with probability  $p_i$ . Formally, each time we draw a vector of binary random variables  $(X_1, X_2 \dots X_N) \sim \pi_{PF}$ ,  $\Pr[i : X_i = 1] = k$  and  $\forall i, \Pr[X_i = 1] = p_i$ .

## 6 Experimental Evaluation

We conduct realistic and synthetic experiments to explore the efficacy and fairness of our probabilistic fair stationary policy. We compare our algorithm **PROBFAIR** with **RISK-AWARE WHITTLE** and naïve fairness-inducing **heuristics** based on the **THRESHOLD WHITTLE** (TW) algorithm.

**RISK-AWARE WHITTLE** incentivizes fairness via concave reward  $r(b)$  [Mate et al., 2021]. We consider the authors' suggested reward function  $r(b) = -e^{\lambda(1-b)}$ ,  $\lambda = 20$ . This imposes a large negative utility on lower belief values, which motivates preemptive intervention. However, as we discuss in the Appendix, **RISK-AWARE WHITTLE** does not guarantee fairness.

We consider three **heuristics** based on **THRESHOLD WHITTLE**: **FIRST**, **LAST**, and **RANDOM**. The heuristics partition the  $k$  pulls available at each timestep into (un)constrained subsets, where a pull is *constrained* if it is executed to satisfy a hard constraint. During constrained pulls, only arms that have not yet been pulled the required number of times within a  $\nu$ -length interval are available; other arms are excluded from consideration, unless *all* arms have already satisfied their constraints. **FIRST**, **LAST**, and **RANDOM** position constrained pulls at the beginning, end, or randomly within each interval of length  $\nu$ , respectively. For each unconstrained pull, the algorithm selects the arm with largest Whittle index according to **THRESHOLD WHITTLE**. Please see Appendix A.4 for pseudocode.

We also compare against the following baseline policies: **ROUND ROBIN**, which selects  $k$  arms to pull in a sequential, round-robin order, and **RANDOM**, which pulls  $k$  arms randomly.

Where applicable, we measure performance in terms of (a) intervention benefit, (b) the price of fairness, and (c) concentration effect. For all simulations, we assign equal value to the adherence of a given patient arm across timesteps. Thus, we set our objective to reward continued adherence: a simple local reward  $r_t(s_t^i) := s_t^i \in \{0, 1\}$  and average reward  $\bar{R}(r(s)) := \frac{1}{T} \sum_{i \in [N]} \sum_{t \in [T]} r(s_t^i)$ .

*Intervention benefit* is the total expected reward of an algorithm, normalized between the reward obtained with no interventions (0% intervention benefit) and the state-of-the-art asymptotically optimal but not fairness inducing **THRESHOLD WHITTLE** algorithm (100%) [Mate et al., 2020]. Formally,

$$\text{IB}_{\text{NoAct, TW}}(\text{ALG}) := \frac{\mathbb{E}_{\text{ALG}}[R(\cdot)] - \mathbb{E}_{\text{NoAct}}[R(\cdot)]}{\mathbb{E}_{\text{TW}}[R(\cdot)] - \mathbb{E}_{\text{NoAct}}[R(\cdot)]} \quad (14)$$

We define the *price of fairness* to be the relative loss in total expected reward associated with following a fairness-enforcing policy, as compared to **THRESHOLD WHITTLE** [Bertsimas et al., 2011]. A small loss ( $\sim 0\%$ ) indicates that fairness has a small impact on total expected reward; conversely, a large loss means total expected reward is sacrificed in order to satisfy the fairness constraints. Formally,

$$\text{PoF}_{\text{TW}}(\text{ALG}) := \frac{\mathbb{E}_{\text{TW}}[R(\cdot)] - \mathbb{E}_{\text{ALG}}[R(\cdot)]}{\mathbb{E}_{\text{TW}}[R(\cdot)]} \quad (15)$$

To measure the *concentration effect*, we use the Herfindahl–Hirschman Index (HHI), a statistical measure of concentration [Rhoades, 1993]. It is useful for measuring the extent to which a small set of arms receive a large proportion of attention due to an unequal distribution of scarce pulls [Hirschman, 1980]. HHI ranges from  $1/N$  to 1; higher values indicate that pulls are concentrated on a small subset of arms.

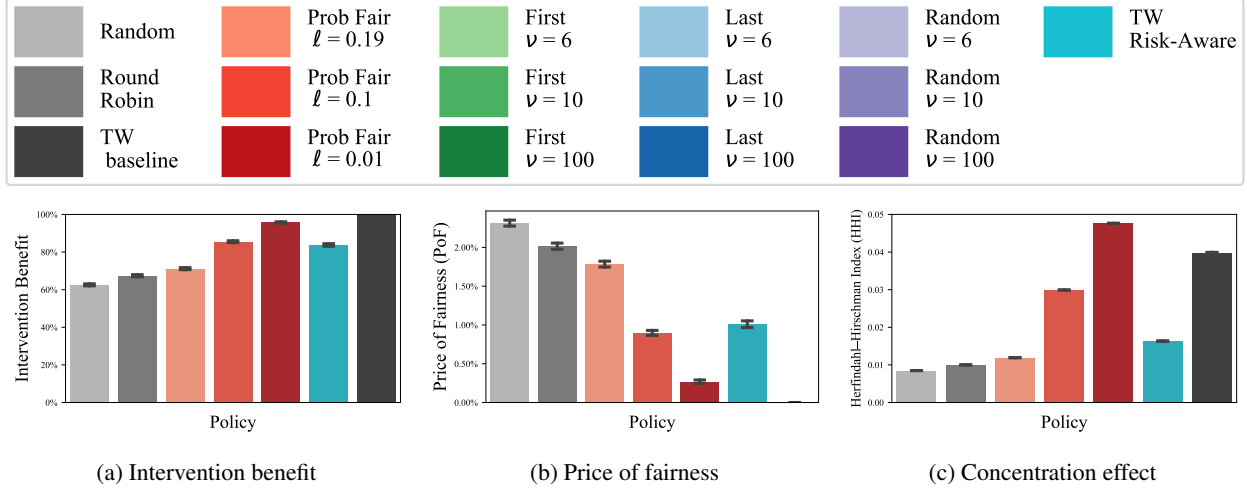
$$\text{HHI}(\text{ALG}) := \sum_{i=1}^N \left( \frac{1}{kT} \sum_{t=1}^T a_t^i \right)^2 \quad (16)$$

## 6.1 Real Data: CPAP Adherence for the Treatment of Obstructive Sleep Apnea

We evaluate how our algorithm might perform in the real world by applying it to a realistic patient adherence behavior model [Kang et al., 2016]. Obstructive sleep apnea (OSA) is a common condition that causes interrupted breathing during sleep [Punjabi, 2008; Young et al., 1993]. In the United States, substantial racial, ethnic, and socioeconomic disparities exist in sleep apnea-related mortality [Kalliny and McKenzie, 2017; Lee et al., 2021]. When used throughout the entirety of sleep, continuous positive airway pressure therapy (CPAP) eliminates nearly 100% of obstructive apneas for the majority of treated patients [Reeves-Hoche et al., 1994; Sawyer et al., 2011; Sullivan et al., 1981]. However, poor adherence behavior in using CPAP reduces its effectiveness and beneficial outcomes. Non-adherence to CPAP therapy is a known common issue among an estimated 30-40% of patients [Rotenberg et al., 2016], and significant disparities in adherence patterns have been shown to exist across racial, age and sex demographics [Borker et al., 2021; Patel et al., 2021; Schwartz et al., 2016].

**Experimental Setup.** We adapt Kang et al. [2016, 2013]’s Markov model of CPAP adherence behavior (a three-state system of hours of nightly CPAP usage) to a two-state system,  $\mathcal{S} = \{0, 1\}$ , where  $s = 1(0)$  represents (non-)adhering to CPAP treatment. The clinical standard for adherence is commonly defined as at least four hours of CPAP machine usage per night [Sawyer et al., 2011]. We randomly initialize the initial state of each arm.

Askland et al. [2020], a review of 41 studies (9,005 participants), identify three types of interventions that promote adherence: educational, supportive, and behavioral interventions. Educational interventions, such as instruction on how to use a CPAP device, are low-cost and ubiquitous. Telemonitoring, phone support, in-home visits, and other forms of supportive interventions are associated with a statistically significant moderate increase in device usage [Fox


 Figure 1:  $\alpha_{\text{intrv}} = 1.1$  and  $T = 180$ , on the CPAP dataset.

et al., 2012; Chervin et al., 1997; Hoy et al., 1999]. Examples of behavioral interventions include motivational enhancement therapy, cognitive behavioral therapy, and myofunctional therapy [Aloia et al., 2013; Olsen et al., 2012; Aloia et al., 2001; Diaferia et al., 2017]. When compared with usual care, behavioral interventions produce a large clinically-meaningful increase in device usage. We consider intervention effects that broadly characterize supportive and behavioral interventions.

Per Kang et al. [2016], we characterize these interventions by their *intervention effect*  $\alpha_{\text{intrv}}$ , defined as the ratio of improvement by intervention,  $P_{s,1}^0 = \alpha_{\text{intrv}} P_{s,1}^1$  for all  $s$ . We consider  $\alpha_{\text{intrv}} = 1.1$  for supportive interventions, because it is estimated that supportive interventions improve nightly CPAP device use by 0.70 hours per night (95% CI 0.36-1.05) [Askland et al., 2020]. Behavioral interventions produce nearly double the nightly device usage (1.31 hrs/night, 95% CI 0.95-1.66), so we set  $\alpha_{\text{intrv}} = 1.2$  [Askland et al., 2020].

We generate  $N = 100$  partially observable arms from these characterizing transition matrices, with added Gaussian noise  $\mathcal{N}(\mu, \sigma^2)$ ,  $\sigma^2 = 0.1$  to cover the breadth of demographics reported in Kang et al. [2013, 2016]. The maximum number of arms that can be pulled is 20% of  $N$ , or  $k = 20$ . We consider two program lengths: one month ( $T = 30$ ) and half a year ( $T = 180$ ).

For fairness, we enforce the probability of a pull  $p_i$  between  $\ell \in [0, \frac{k}{N} = 0.2]$  and  $u = 1$ , for all arms  $i$ . We set  $\ell = 0.01, 0.1, 0.19$ ; these values of  $\ell$  roughly correspond to one pull per (100, 10, 6)-length interval  $\nu$ , which allows us to compare our algorithm with the heuristic algorithms described above. Throughout this section, we compute the  $p_i$ 's in PROBFAIR with a linear programming approximation approach. Another efficient approach with  $\epsilon$ -bounded guarantees is given in Section 5.2.

**Results.** All results shown are bootstrapped over 500 iterations; the plots have error bars for 95% confidence intervals (CI). The legend in Figure 1 applies for all plots.

Figure 1 shows results for moderate intervention effect  $\alpha_{\text{intrv}} = 1.1$  and horizon  $T = 180$ . PROBFAIR maintains a similar intervention benefit as RISK-AWARE WHITTLE (Fig. 1a) with better price of fairness (Fig. 1b) but poorer concentration effect (Fig. 1c) across fairness constraint selections  $\ell$ . However, for a larger intervention effect  $\alpha_{\text{intrv}} = 1.2$ , PROBFAIR has a better concentration effect while the intervention benefit remains comparable (Refer to Appendix A.5.3 for extended results.). Recall that the intervention benefit is normalized; the absolute reward is higher in the latter case.

PROBFAIR produces comparable or better intervention benefit under probabilistic constraints ( $\ell \in [0.19, 0.1, 0.01]$ ) versus heuristics enforcing hard integer periodicity constraints ( $\nu = [6, 10, 100]$ ) (Fig. 2). Simulations with a smaller horizon  $T = 30$  produce similar results (Appendix A.5.3).

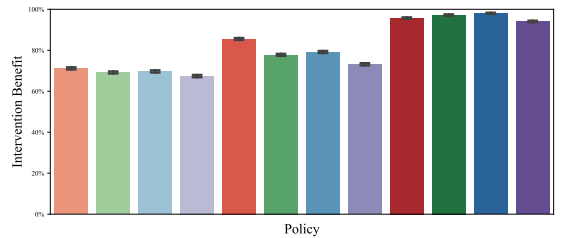
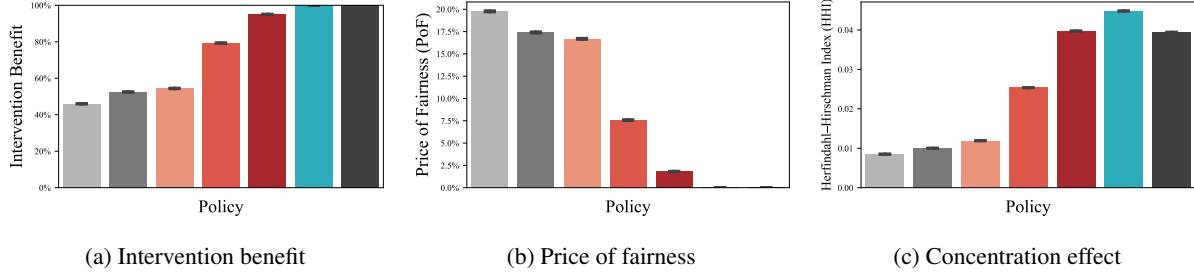


Figure 2: Intervention benefit, vs heuristics




 Figure 3:  $N = 100$  randomly generated arms,  $T = 180$ .

## 6.2 Synthetic Data

In addition, we evaluate our algorithm under a more general set of transition matrices. We consider a cohort of randomly generated arms such that the structural constraints outlined in Section 2.1 are preserved. In Appendix A.5.2, we provide results for three additional cohorts: *forward (reverse)*, randomly generated from the set of possible forward (reverse) threshold optimal arms, respectively, and *mixed*, generated with half of arms forward threshold optimal and half reverse threshold optimal. We set the initial state,  $s_0^i = 1 \forall i \in [N]$ .

**Results.** The intervention benefit of PROBFAIR is comparable to RISK-AWARE WHITTLE and THRESHOLD WHITTLE (Fig. 3a). Interestingly, the intervention benefit of our stationary policy consistently outperforms all tested heuristics for intermediate values of  $\ell$  (Fig. 4, Appendix A.5). The HHI index of PROBFAIR is lower than that of RISK-AWARE WHITTLE and THRESHOLD WHITTLE, that is, arm pulls are allocated more equitably (Fig. 3c). We note that RISK-AWARE WHITTLE is *strictly worse* than THRESHOLD WHITTLE in these results—it obtains nearly the same utility (Fig. 3a) and therefore 0% price of fairness, but its concentration effect is *greater* than its strictly utilitarian counterpart.

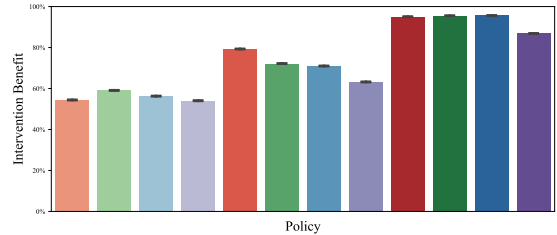


Figure 4: Intervention benefit, vs heuristics

## 7 Conclusion & Future Research

The constrained resource allocation algorithm we present reflects two competing societal objectives: maximization of overall welfare and individual fairness. The acceptability of this trade-off will depend in part on extenuating clinical circumstances, including: (1) the estimated variance in marginal benefit associated with receiving the intervention; and (2) the presence of alternatives to which attention-starved patients could be “re-routed”. Additionally, in settings where transition matrices must be estimated or learned from patient characteristics, it will be important to consider whether estimation errors are positively correlated with protected attributes, to mitigate the risk of algorithmic bias.

## 8 Acknowledgements

Christine Herlihy was supported by the National Institute of Standards and Technology’s (NIST) Professional Research Experience Program (PREP). John Dickerson and Aviva Prins were supported in part by NSF CAREER Award IIS-1846237, NSF D-ISEN Award #2039862, NSF Award CCF-1852352, NIH R01 Award NLM-013039-01, NIST MSE Award #20126334, DARPA GARD #HR00112020007, DoD WHS Award #HQ003420F0035, and a Google Faculty Research award. Aravind Srinivasan was supported in part by NSF awards CCF-1749864 and CCF-1918749, as well as research awards from Adobe, Amazon, and Google. The views and conclusions contained in this publication are those of the authors and should not be interpreted as representing official policies or endorsements of U.S. government or funding agencies. We thank Samuel Dooley, Dr. Furong Huang, Naveen Raman, and Daniel Smolyak for helpful input and feedback.

## References

- Mark S Aloia, Lina Di Dio, Nora Ilniczky, Michael L Perlis, Donald W Greenblatt, and Donna E Giles. Improving compliance with nasal CPAP and vigilance in older adults with OSAHS. *Sleep and Breathing*, 5(1):13–21, 2001.
- Mark S Aloia, J Todd Arnedt, Matthew Strand, Richard P Millman, and Belinda Borrelli. Motivational Enhancement to Improve Adherence to Positive Airway Pressure in Patients with Obstructive Sleep Apnea: a Randomized Controlled Trial. *Sleep*, 36(11):1655–1662, 2013.
- Kathleen Askland, Lauren Wright, Dariusz R Wozniak, Talia Emmanuel, Jessica Caston, and Ian Smith. Educational, Supportive and Behavioural Interventions to Improve Usage of Continuous Positive Airway Pressure Machines in Adults with Obstructive Sleep Apnoea. *Cochrane Database of Systematic Reviews*, (4), 2020.
- Turgay Ayer, Can Zhang, Anthony Bonifonte, Anne C Spaulding, and Jagpreet Chhatwal. Prioritizing Hepatitis C Treatment in US Prisons. *Operations Research*, 67(3):853–873, 2019.
- Jeremy Bentham. An Introduction to the Principles of Morals and Legislation. Technical report, McMaster University Archive for the History of Economic Thought, 1781.
- Dimitris Bertsimas, Vivek F Farias, and Nikolaos Trichakis. The Price of Fairness. *Operations research*, 59(1):17–31, 2011.
- Priya V Borker, Emely Carmona, Utibe R Essien, Gul Jana Saeed, S Mehdi Nouraie, Jessie P Bakker, Christy J Stitt, Mark S Aloia, and Sanjay R Patel. Neighborhoods with greater prevalence of minority residents have lower cpap adherence. *American Journal of Respiratory and Critical Care Medicine*, (ja), 2021.
- Yifang Chen, Alex Cuellar, Haipeng Luo, Jignesh Modi, Heramb Nemlekar, and Stefanos Nikolaidis. Fair Contextual Multi-Armed Bandits: Theory and Experiments. volume 124 of *Proceedings of Machine Learning Research*, pages 181–190, Virtual, 03–06 Aug 2020. PMLR. URL <http://proceedings.mlr.press/v124/chen20a.html>.
- Ronald D Chervin, Sarah Theut, Claudio Bassetti, and Michael S Aldrich. Compliance With Nasal CPAP Can Be Improved by Simple Interventions. *Sleep*, 20(4):284–289, 1997.
- Maria De-Arteaga, Riccardo Fogliato, and Alexandra Chouldechova. A Case for Humans-in-the-Loop: Decisions in the Presence of Erroneous Algorithmic Scores. In *Proceedings of the 2020 CHI Conference on Human Factors in Computing Systems*, pages 1–12, 2020.
- Giovana Diaféria, Rogerio Santos-Silva, Eveli Truksinas, Fernanda LM Haddad, Renata Santos, Silvana Bommarito, Luiz C Gregório, Sergio Tufik, and Lia Bittencourt. Myofunctional therapy improves adherence to continuous positive airway pressure treatment. *Sleep and Breathing*, 21(2):387–395, 2017.
- Berkeley J Dietvorst, Joseph P Simmons, and Cade Massey. Algorithm aversion: People erroneously avoid algorithms after seeing them err. *Journal of Experimental Psychology: General*, 144(1):114, 2015.
- Nurit Fox, AJ Hirsch-Allen, Elizabeth Goodfellow, Joshua Wenner, John Fleetham, C Frank Ryan, Mila Kwiatkowska, and Najib T Ayas. The Impact of a Telemedicine Monitoring System on Positive Airway Pressure Adherence in Patients with Obstructive Sleep Apnea: A Randomized Controlled Trial. *Sleep*, 35(4):477–481, 2012.
- Alain Ghouila-Houri. Caractérisation des matrices totalement unimodulaires. *Comptes Rendus Hebdomadaires des Séances de l'Académie des Sciences (Paris)*, 254:1192–1194, 1962.
- Albert O Hirschman. *National Power and the Structure of Foreign Trade*, volume 105. Univ of California Press, 1980.
- Carol J Hoy, Marjorie Vennelle, Ruth N Kingshott, Heather M Engleman, and Neil J Douglas. Can Intensive Support Improve Continuous Positive Airway Pressure Use in Patients with the Sleep Apnea/Hypopnea Syndrome? *American Journal of Respiratory and Critical Care Medicine*, 159(4):1096–1100, 1999.
- Matthew Joseph, Michael Kearns, Jamie H Morgenstern, and Aaron Roth. Fairness in Learning: Classic and Contextual Bandits. In D. D. Lee, M. Sugiyama, U. V. Luxburg, I. Guyon, and R. Garnett, editors, *Advances in Neural Information Processing Systems 29*, pages 325–333. Curran Associates, Inc., 2016. URL <http://papers.nips.cc/paper/6355-fairness-in-learning-classic-and-contextual-bandits.pdf>.
- Young Hun Jung and Ambuj Tewari. Regret Bounds for Thompson Sampling in Episodic Restless Bandit Problems. In H. Wallach, H. Larochelle, A. Beygelzimer, F. d'Alché-Buc, E. Fox, and R. Garnett, editors, *Advances in Neural Information Processing Systems 32*, pages 9007–9016. Curran Associates, Inc., 2019. URL <http://papers.nips.cc/paper/9102-regret-bounds-for-thompson-sampling-in-episodic-restless-bandit-problems.pdf>.
- Medhat Kalliny and Judith Green McKenzie. Occupational health and sleep issues in underserved populations. *Primary Care: Clinics in Office Practice*, 44(1):e73–e97, 2017.

- Yuncheol Kang, Vittaldas V Prabhu, Amy M Sawyer, and Paul M Griffin. Markov models for treatment adherence in obstructive sleep apnea. *Age*, 49:11–6, 2013.
- Yuncheol Kang, Amy M Sawyer, Paul M Griffin, and Vittaldas V Prabhu. Modelling Adherence Behaviour for the Treatment of Obstructive Sleep Apnoea. *European journal of operational research*, 249(3):1005–1013, 2016.
- Christopher J Kelly, Alan Karthikesalingam, Mustafa Suleyman, Greg Corrado, and Dominic King. Key Challenges for Delivering Clinical Impact with Artificial Intelligence. *BMC medicine*, 17(1):195, 2019.
- Y-C Lee, K-Y Chang, AF Monegro, and MJ Mador. Racial disparity in sleep apnea-related mortality in the united states. In *TP21. TP021 THE IMPACT OF LUNG DISEASE AMONG UNDERSERVED POPULATIONS*, pages A1744–A1744. American Thoracic Society, 2021.
- Fengjiao Li, Jia Liu, and Bo Ji. Combinatorial Sleeping Bandits with Fairness Constraints. *CoRR*, abs/1901.04891, 2019. URL <http://arxiv.org/abs/1901.04891>.
- Keqin Liu and Qing Zhao. Indexability of Restless Bandit Problems and Optimality of Whittle Index for Dynamic Multichannel Access. *IEEE Transactions on Information Theory*, 56(11):5547–5567, Nov 2010. ISSN 1557-9654. doi: 10.1109/tit.2010.2068950. URL <http://dx.doi.org/10.1109/TIT.2010.2068950>.
- Elliot Marseille and James G. Kahn. Utilitarianism and the Ethical Foundations of Cost-Effectiveness Analysis in Resource Allocation for Global Health. *Philosophy, Ethics, and Humanities in Medicine*, 14(1):1–7, 2019. doi: 10.1186/s13010-019-0074-7.
- Aditya Mate, Jackson Killian, Haifeng Xu, Andrew Perrault, and Milind Tambe. Collapsing Bandits and Their Application to Public Health Intervention. *Advances in Neural Information Processing Systems*, 33, 2020.
- Aditya Mate, Andrew Perrault, and Milind Tambe. Risk-Aware Interventions in Public Health: Planning with Restless Multi-Armed Bandits. In *20th International Conference on Autonomous Agents and Multiagent Systems (AAMAS)*, London, UK, 2021.
- José Niño-Mora. A Verification Theorem for Threshold-Indexability of Real-State Discounted Restless Bandits. *Mathematics of Operations Research*, 45(2):465–496, 2020.
- Sara Olsen, Simon S Smith, Tian PS Oei, and James Douglas. Motivational interviewing (MINT) improves continuous positive airway pressure (CPAP) acceptance and adherence: a randomized controlled trial. *Journal of consulting and clinical psychology*, 80(1):151, 2012.
- Christos H Papadimitriou and John N Tsitsiklis. The Complexity of Optimal Queueing Network Control. In *Proceedings of IEEE 9th Annual Conference on Structure in Complexity Theory*, pages 318–322. IEEE, 1994.
- Sanjay R Patel, Jessie P Bakker, Christy J Stitt, Mark S Aloia, and S Mehdi Nouraie. Age and sex disparities in adherence to cpap. *Chest*, 159(1):382–389, 2021.
- Aviva Prins, Aditya Mate, Jackson A Killian, Rediet Abebe, and Milind Tambe. Incorporating Healthcare Motivated Constraints in Restless Bandit Based Resource Allocation. *preprint*, 2020. URL <https://teamcore.seas.harvard.edu/publications/incorporating-healthcare-motivated-constraints-restless-bandit-based-resource>.
- Naresh M Punjabi. The epidemiology of adult obstructive sleep apnea. *Proceedings of the American Thoracic Society*, 5(2):136–143, 2008.
- Alvin Rajkomar, Michaela Hardt, Michael D Howell, Greg Corrado, and Marshall H Chin. Ensuring Fairness in Machine Learning to Advance Health Equity. *Annals of internal medicine*, 169(12):866–872, 2018.
- John Rawls. *A Theory of Justice*. Belknap Press of Harvard University Press, Cambridge, Massachusetts, 1 edition, 1971. ISBN 0-674-88014-5.
- Mary Kathryn Reeves-Hoche, Raymond Meck, and Clifford W Zwillich. Nasal cpap: an objective evaluation of patient compliance. *American Journal of Respiratory and Critical Care Medicine*, 149(1):149–154, 1994.
- Stephen A Rhoades. The Herfindahl-Hirschman Index. *Fed. Res. Bull.*, 79:188, 1993.
- Brian W Rotenberg, Dorian Murariu, and Kenny P Pang. Trends in CPAP adherence over twenty years of data collection: a flattened curve. *Journal of Otolaryngology-Head & Neck Surgery*, 45(1):1–9, 2016.
- Amy M Sawyer, Nalaka S Gooneratne, Carole L Marcus, Dafna Ofer, Kathy C Richards, and Terri E Weaver. A systematic review of CPAP adherence across age groups: clinical and empiric insights for developing CPAP adherence interventions. *Sleep medicine reviews*, 15(6):343–356, 2011.
- Leslie Scheunemann and Douglas White. The Ethics and Reality of Rationing in Medicine. *Chest*, 140:1625–32, 12 2011. doi: 10.1378/chest.11-0622.

- Skai W Schwartz, Yuri Sebastião, Julie Rosas, Michelle R Iannacone, Philip R Foulis, and W McDowell Anderson. Racial disparity in adherence to positive airway pressure among us veterans. *Sleep and Breathing*, 20(3):947–955, 2016.
- A. Srinivasan. Distributions on Level-Sets with Applications to Approximation Algorithms. In *Proceedings of the 42nd IEEE Symposium on Foundations of Computer Science*, FOCS '01, page 588, USA, 2001. IEEE Computer Society. ISBN 0769513905.
- Lauren N. Steimle and Brian T. Denton. *Markov Decision Processes for Screening and Treatment of Chronic Diseases*, pages 189–222. Springer International Publishing, Cham, 2017. ISBN 978-3-319-47766-4. doi: 10.1007/978-3-319-47766-4\_6. URL [https://doi.org/10.1007/978-3-319-47766-4\\_6](https://doi.org/10.1007/978-3-319-47766-4_6).
- ColinE Sullivan, Michael Berthon-Jones, FaiqG Issa, and Lorraine Eves. Reversal of obstructive sleep apnoea by continuous positive airway pressure applied through the nares. *The Lancet*, 317(8225):862–865, 1981.
- Richard R Weber and Gideon Weiss. On an Index Policy for Restless Bandits. *Journal of Applied Probability*, pages 637–648, 1990.
- Peter Whittle. Restless Bandits: Activity Allocation in a Changing World. *Journal of applied probability*, 25(A): 287–298, 1988.
- Terry Young, Mari Palta, Jerome Dempsey, James Skatrud, Steven Weber, and Safwan Badr. The occurrence of sleep-disordered breathing among middle-aged adults. *New England Journal of Medicine*, 328(17):1230–1235, 1993.

## A Appendix

### A.1 Notation

In Table 1, we present an overview of the notation used in the paper.  $[N]$  denotes the set  $\{1, 2, \dots, N\}$ .

Table 1: Notation used in our model and notes on their interpretation.

<b>MDP Variables</b> Here, timestep $t \in [T] = \{1, 2, \dots, T\}$ (subscript) and arm index $i \in [N] = \{1, 2, \dots, N\}$ (superscript) are implied.		
State space	$s \in \mathcal{S} = \{0, 1\}$	$s = \begin{cases} 1 & \text{arm is in the 'good' state.} \\ 0 & \text{else} \end{cases}$
Belief space	$b \in \mathcal{B} = [0, 1]$ $b_{t+1} = \begin{cases} s_{t+1} & \text{if known} \\ b_t P_{1,1}^0 + (1 - b_t) P_{0,1}^0 & \text{else} \end{cases}$	If an arm's true state is unknown, the recursive belief state approximates it.
Action space	$a \in \mathcal{A} = \{0, 1\}$	$a = \begin{cases} 1 & \text{pull arm (i.e., provide intervention)} \\ 0 & \text{else, don't pull} \end{cases}$
<b>MDP Functions</b>		
Transition function	$P: \mathcal{S} \times \mathcal{A} \times \mathcal{S} \rightarrow [0, 1]$ $s_t, a_t, s_{t+1} \mapsto \Pr(s_{t+1}   s_t, a_t)$	The probability of an arm going from state $s_t$ to $s_{t+1}$ , given action $a_t$ . Equivalent (matrix) notation: $P_{s_t, s_{t+1}}^{a_t}$ .
Reward function	$r: \mathcal{S} \text{ or } \mathcal{B} \rightarrow \mathbb{R}$	$r(b)$ is used in computing the Whittle index.
Policy function	$\pi: \mathcal{S} \rightarrow \mathcal{A}$	A policy for actions. The set of optimal policies is $\pi^* \in \Pi^*$ .
<b>RMAB Variables</b>		
Timestep	$\{t \in \mathbb{Z}^+ \mid t \leq T\}$	This timestep is implicit in the MDP.
Arm index	$i \in \{1, 2, \dots, N\}$	Each arm can represent a patient. $k$ arms can be called at any timestep $t$ .
<b>Objective Functions</b> Objective: find a policy $\pi^* = \max_{\pi} \mathbb{E}_{\pi}[R(\cdot)]$ .		
Discounted reward function	$R_{\beta}^{\pi}: \mathcal{S}^N \rightarrow \mathbb{R}$ $s_0^1, s_0^2, \dots, s_0^N \mapsto \sum_{i \in [N]} \sum_{t \in [T]} \beta^t r(s_t^i)$	$\beta \in [0, 1]$ is some <i>discount parameter</i> .
Average reward function	$\bar{R}^{\pi}: \mathcal{S}^N \rightarrow \mathbb{R}$ $s_0^1, s_0^2, \dots, s_0^N \mapsto \frac{1}{T} \sum_{i \in [N]} \sum_{t \in [T]} r(s_t^i)$	
<b>Constraint Functions</b>		
Hard integer periodicity constraint	$\bigwedge_{j=0}^{\lceil \frac{T}{\nu} \rceil} \sum_{t=j\nu+1}^{(j+1)\nu} a_t^i \geq 1$	Guarantee arm $i$ is pulled at least once within each period of $\nu$ timesteps.
Probabilistic constraint	$\bigwedge_{i \in [N]} \bigwedge_{t \in [T]} \Pr(a_t^i = 1 \mid i, t) \in [\ell, u]$	Pull each arm with probability $p_i \in [\ell, u]$ , where $\ell \in (0, \frac{k}{N}]$ and $u \in [\frac{k}{N}, 1]$ .
Minimum selection fraction constraint	$\bigwedge_{i \in [N]} \frac{1}{T} \sum_{t=1}^T a_t^i \geq \psi$	Arm $i$ should be pulled at least some minimum fraction $\psi \in (0, 1)$ of timesteps.

### A.2 Integer Program Formulation

In this section, we present an integer program (IP) that maximizes total expected reward under both budget *and* hard equity constraints, for problem instances with feasible hyperparameters. First, we formulate the IP. Then we discuss the objective function coefficients. Finally, we prove that any problem instance with feasible hyperparameters yields a totally unimodular (TU) constraint matrix, which ensures that the linear program (LP) relaxation of our IP will yield an integral solution.

The solution to the IP is the policy  $\vec{x} \in \{0, 1\}^{N|A|T}$ . Each  $x_{i,a,t}$  in this IP is a binary decision variable that represents whether or not we take action  $a$  for arm  $i$  at timestep  $t$ .

To define the objective function, recall that the agent seeks to maximize total expected reward,  $\mathbb{E}_\pi[R(\cdot)]$ . For clarity of exposition, we specifically consider the linear global reward function  $R(r(s)) = \sum_{i=1}^N \sum_{t=0}^T s_t^i$ . Note that we remove the  $1/T$  normalization for clarity of exposition and that this implies the discount rate,  $\beta = 1$ ; however, the approach outlined here can be extended in a straightforward manner for  $\beta \in (0, 1)$ . In order to compute the expected reward associated with taking action  $a$  for arm  $i$  at time  $t$ , we must consider: (1) what state is the arm currently in (i.e., what is the realized value of  $s_t^i \in \{0, 1\}$ )? (2) when the arm transitions from  $s_t$  to  $s_{t+1}$  by virtue of taking action  $a$ , what reward,  $r(\cdot)$ , should we expect to earn?

Because we define  $r(s) = s$ , (2) can be reframed as: what is the probability  $p(s_{t+1} = 1 | s_t^i, a_t^i)$  that action  $a$  causes a transition from  $s_t$  to the adherent state? Because each arm's state at time  $t$  is stochastic, depending not only on the sequence of actions taken in previous timesteps, but the associated set of stochastic transitions informed by the arm's underlying MDP, each coefficient of our objective function must be computed as the expectation over the possible values of  $s_t \in S$ :

$$\vec{c} = \mathbb{E}_s[p(s_{t+1} = 1 | x_{i,a,t}, s_t)] \quad \forall i, a, t \in [N] \times \mathcal{A} \times [T] \quad (\text{A.1})$$

$$= \frac{1}{2^t} \sum_{s \in S} p(s_t = s) \sum_{s' \in S} p(s_{t+1} = s' | x_{i,a,t}, s_t = s) r(s') \quad \forall i, a, t \in [N] \times \mathcal{A} \times [T] \quad (\text{A.2})$$

$$= \frac{1}{2^t} \sum_{s \in S} p(s_t = s) p(r(s_{t+1}) = 1 | x_{i,a,t}, s_t = s) \quad \forall i, a, t \in [N] \times \mathcal{A} \times [T] \quad (\text{A.3})$$

$$= \frac{1}{2^t} \sum_{s \in S} p(s_t = s) p(s_{t+1} = 1 | x_{i,a,t}, s_t = s) \quad \forall i, a, t \in [N] \times \mathcal{A} \times [T] \quad (\text{A.4})$$

The resulting integer program is given by:

$$\begin{aligned} \max \quad & c^T x & (\text{A.5}) \\ \text{s.t.} \quad & \sum_{a=1}^{|A|} x_{i,a,t} = 1 & \forall i \in [N], t \in [T] \quad (\text{a) Select exactly one action per arm } i \text{ at each } t \\ \text{if int. per:} \quad & \sum_{t \in I_j} x_{i,1,t} \geq 1 & \forall j \in \left\{ 0, 1, \dots, \frac{T-\nu}{\nu} \right\} \quad (\text{b.i) Pull each arm } i \text{ at least once during each interval of length } \nu \\ \text{if min. sel:} \quad & \frac{1}{T} \sum_{t=1}^T x_{i,1,t} \geq \psi & \psi \in (0, 1), \forall i \in N \quad (\text{b.ii) Pull each arm } i \text{ at least a minimum fraction } \psi \text{ of } T \text{ rounds} \\ & \sum_{i=1}^N x_{i,1,t} = k & \forall t \in [T] \quad (\text{c) Pull exactly } k \text{ arms at each } t \\ & x_{i,a,t} \in \{0, 1\} & \forall i \in [N], a \in \mathcal{A}, t \in [T] \quad (\text{d) Each arm-action-timestep choice is a binary decision variable} \end{aligned}$$

We present experimental results using this IP in Appendix A.5.2.

### A.2.1 Estimation of Objective Function Coefficients

The key challenge we encounter when we seek to enumerate the IP outlined in the previous section is that exact computation of the objective function coefficients,  $\vec{c} \in \mathbb{R}^{N|A|T}$  is intractable. Each arm contributes  $A \times T$  coefficients, and while calculation is trivially parallelizable over arms, we must consider a probability tree like the one depicted in Figure 5 for each arm.

The number of decision variables required to enumerate each arm's game tree is of order  $O(|S||A|^T)$  and there are  $N$  such trees, so even a linear program (LP) relaxation is not tractable for larger values of  $T$  and  $N$ , which motivates us to propose the probabilistically fair stationary policy (Section 5) as an efficient alternative.

**Example 1** Suppose we wish to find the coefficient  $c'$  corresponding to  $x_{i,a=0,t=2}$ . From Equation A.4, we have  $c' = \frac{1}{2^2} \sum_{s \in S} p(s_2 = s) p(s_3 = 1 | x_{i,a=0,t=2}, s_2 = s)$ . Equivalently, we sum the weight of each path from the root



node to the highlighted end nodes in Figure 5 and normalize by  $\frac{1}{2^2}$ :

$$\begin{aligned}
 c' = \frac{1}{4} & \left( P_{s_0,0}^0 P_{0,0}^0 P_{0,1}^0 + P_{s_0,0}^0 P_{0,0}^1 P_{0,1}^0 + P_{s_0,0}^0 P_{0,1}^0 P_{1,1}^0 + P_{s_0,0}^0 P_{0,1}^1 P_{1,1}^0 \right. \\
 & + P_{s_0,0}^1 P_{0,0}^0 P_{0,1}^0 + P_{s_0,0}^1 P_{0,0}^1 P_{0,1}^0 + P_{s_0,0}^1 P_{0,1}^0 P_{1,1}^0 + P_{s_0,0}^1 P_{0,1}^1 P_{1,1}^0 \\
 & \left. + \dots \right) \quad \text{For each of the } (|\mathcal{A}||\mathcal{S}|)^t = 16 \text{ paths to a blue node in Figure 5.}
 \end{aligned} \tag{A.6}$$

## A.2.2 LP Relaxation and Integrality of Solution

Our proof leverages a theorem introduced by Ghouila-Houri and restated below for convenience, which can be used to determine whether a matrix,  $A \in \mathbb{R}^{m \times n}$  is totally unimodular:

**Lemma A.1** (Ghouila-Houri [1962]) *A matrix  $A \in \mathbb{Z}^{m \times n}$  is totally unimodular (TU) if and only if for every subset of the rows  $R \subseteq [m]$ , there is a partition  $R = R_1 \cup R_2$  such that for every  $j \in [n]$ ,*

$$\sum_{i \in R_1} A_{ij} - \sum_{i \in R_2} A_{ij} \in \{-1, 0, 1\} \tag{A.7}$$

**Theorem A.2** *Within the context of the integer program outlined in Appendix A.2, any feasible problem instance will produce a constraint matrix that is totally unimodular (TU).*

**PROOF** To begin, we establish the dimensions of any such constraint matrix  $\mathbf{A}$  and note the maximum possible column-wise sum that each of its component submatrices may contribute. Note that equity constraint (b.ii), which requires the agent to pull each arm  $i$  at least a minimum fraction,  $\psi \in (0, 1)$ , of  $T$  rounds, can be thought of as a special case of the integer periodicity equity constraint (b.i), where  $\nu = T$  and each arm must be pulled at least  $\lceil T\psi \rceil$  times. As such, we assume that at most one of the hard fairness constraints can be selected, and focus on the more general of the two, which is the integer periodicity constraint. For notational convenience, we refer to constraints by their alphabetic identifiers, let (b) stand in for (b.i), and define a function  $\varphi : r \in \mathbf{R} \subseteq \mathbf{A} \mapsto e \in \{a, b, c\}$  that maps each row to its corresponding constraint type.

First, recall that each  $x_{i,a,t}$  represents a single binary decision variable, and corresponds to a column in  $\mathbf{A}$ . There are  $N \times |\mathcal{A}| \times T$  such columns. Next, note that constraint (a) enforces the requirement that we select *exactly* one action per arm per timestep. Formally,  $\forall i, t \in N \times T, \exists! a \in \mathcal{A}$  s.t.  $x_{i,a,t} = 1$ . Correspondingly,  $\forall a' \in \mathcal{A} \setminus a, x_{i,a',t} = 0$ . The column vectors of the associated sub-matrix,  $\mathbf{A}_a \in \mathbb{Z}^{NT \times N|\mathcal{A}|T}$ , are indexed by disjoint  $(i, a, t) \in N \times |\mathcal{A}| \times T$ ; thus, each column vector contains a single non-zero entry and for  $\mathbf{R}_a \subseteq \mathbf{A}_a$ , taking the column-wise sum will yield a vector  $\vec{v} \in \mathbb{Z}^{N|\mathcal{A}|T}$  with every entry equal to 1.

In a similar vein, equity constraint (b) enforces the requirement that we must pull each arm,  $i$  at least once during each interval  $I_j$  of length  $\nu_i$ . Within the associated sub-matrix,  $\mathbf{A}_b \in \mathbb{Z}^{N\lceil \frac{T}{\nu_i} \rceil \times N|\mathcal{A}|T}$ , each column that corresponds to a passive action (e.g.,  $x_{i,a=0,t}$ ) will have *only* zero-valued entries, since passive action decision variables are not impacted by constraint (b). Conversely, each column that corresponds to an active action (e.g.,  $x_{i,a=1,t}$ ) will have a single non-zero entry. Each active action column corresponding to a specific arm-timestep can be mapped to exactly one interval. Thus, for  $\mathbf{R}_b \subseteq \mathbf{A}_b$ , taking the column-wise sum will yield a vector  $\vec{v} \in \mathbb{Z}^{N|\mathcal{A}|T}$  with every entry taking a value  $\in \{0, 1\}$ .

The budget constraint (c) enforces the requirement that we must pull exactly  $k$  of the  $N$  arms at each timestep. Much like equity constraint (b), only columns corresponding to active actions are impacted. Thus, within the associated sub-matrix,  $\mathbf{A}_c \in \mathbb{Z}^{T \times N|\mathcal{A}|T}$ , each column that corresponds to a passive action (e.g.,  $x_{i,a=0,t}$ ) will have *only* zero-valued entries, while each column that corresponds to an active action (e.g.,  $x_{i,a=1,t}$ ) can be mapped to a single timestep, and will have a single non-zero entry. Thus, for  $\mathbf{R}_c \subseteq \mathbf{A}_c$ , taking the column-wise sum also yield a vector  $\vec{v} \in \mathbb{Z}^{N|\mathcal{A}|T}$  with every entry taking a value  $\in \{0, 1\}$ .

The complete constraint matrix  $\mathbf{A}$  thus contains  $NT + N\lceil \frac{T}{\nu_i} \rceil + T$  rows. Three possible cases arise when we consider every subset of these rows: (1)  $\mathbf{R} \subsetneq \mathbf{A} = \emptyset$ ; (2)  $\mathbf{R} \subsetneq \mathbf{A}; \mathbf{R} \cap \mathbf{A} \neq \emptyset$ ; (3)  $\mathbf{R} \subseteq \mathbf{A}$ .

**Case 1**  $\mathbf{R} \subsetneq \mathbf{A} = \emptyset$ . To satisfy Lemma A.1, partition  $\mathbf{R}$  such that  $\mathbf{R} = \mathbf{R}_1 \cup \mathbf{R}_2 = \emptyset \cup \emptyset$ . Then, for every  $j \in [n]$ ,

$$\sum_{i \in \mathbf{R}_1} \mathbf{A}_{ij} - \sum_{i \in \mathbf{R}_2} \mathbf{A}_{ij} = 0 - 0; 0 \in \{-1, 0, 1\} \blacksquare$$

**Case 2**  $\mathbf{R} \subsetneq \mathbf{A}; \mathbf{R} \cap \mathbf{A} \neq \emptyset$ . If we consider  $\cup_{r \in \mathbf{R}} \varphi(r)$ , there are  $\sum_{k=1}^3 \binom{3}{k}$  possible sets of observed constraint types:  $\{a\} \vee \{b\} \vee \{c\} \vee \{a, b\} \vee \{a, c\} \vee \{b, c\} \vee \{a, b, c\}$ .



1. If  $|\cup_{r \in \mathbf{R}} \varphi(r)| = 1$ , then any partition of  $\mathbf{R}$  will satisfy Lemma A.1. Without loss of generality, let each row  $r \in \mathbf{R}$  belong to  $\mathbf{R}_1$  and  $\mathbf{R}_2 = \emptyset$ .

i. If  $\cup_{r \in \mathbf{R}} \varphi(r) = \{a\}$ , taking the column-wise sum of  $\mathbf{R}_1$  will yield a vector  $\vec{v} \in \mathbb{Z}^{N|\mathcal{A}|T}$  with every entry  $\in \{1\}$  if  $\mathbf{R} \subseteq \mathbf{A}_a$ , and  $\in \{0, 1\}$  otherwise. Thus,  $\forall j \in [N|\mathcal{A}|T]$ ,

$$\sum_{i \in \mathbf{R}_1} \mathbf{A}_{ij} - \sum_{i \in \mathbf{R}_2} \mathbf{A}_{ij} = 0 - 0 \vee 1 - 0; \{0, 1\} \subsetneq \{-1, 0, 1\} \blacksquare$$

ii. If  $\cup_{r \in \mathbf{R}} \varphi(r) = \{b\} \vee \{c\}$ , taking the column-wise sum of  $\mathbf{R}_1$  will yield a vector  $\vec{v} \in \mathbb{Z}^{N|\mathcal{A}|T}$  with every entry corresponding to a passive action column  $\in \{0\}$  and every entry corresponding to an active action column  $\in \{1\}$  if  $\mathbf{R} \subseteq \mathbf{A}_{b \vee c}$ , and  $\in \{0, 1\}$  otherwise. Thus,  $\forall j \in [N|\mathcal{A}|T]$ ,

$$\sum_{i \in \mathbf{R}_1} \mathbf{A}_{ij} - \sum_{i \in \mathbf{R}_2} \mathbf{A}_{ij} = 0 - 0 \vee 1 - 0; \{0, 1\} \subsetneq \{-1, 0, 1\} \blacksquare$$

2. If  $|\cup_{r \in \mathbf{R}} \varphi(r)| = 2$ , without loss of generality, partition as follows: sort the elements  $\in \cup_{r \in \mathbf{R}} \varphi(r)$  lexicographically, and let  $\mathbf{R}_1 = \{r | \varphi(r) = \min \cup_{r \in \mathbf{R}} \varphi(r)\}$  and  $\mathbf{R}_2 = \mathbf{R} \setminus \mathbf{R}_1$ . Per Case 2.1 (i) and (ii), taking the column-wise sums of  $\mathbf{R}_1$  and  $\mathbf{R}_2$  will yield two vectors,  $\vec{v}_1, \vec{v}_2 \in \mathbb{Z}^{N|\mathcal{A}|T}$ , each of which will contain only entries  $\in \{0, 1\}$ . Thus,  $\forall j \in [N|\mathcal{A}|T]$ ,

$$\sum_{i \in \mathbf{R}_1} \mathbf{A}_{ij} - \sum_{i \in \mathbf{R}_2} \mathbf{A}_{ij} = 0 - 0 \vee 0 - 1 \vee 1 - 0 \vee 1 - 1; \{-1, 0, 1\} \subseteq \{-1, 0, 1\} \blacksquare$$

3. If  $|\cup_{r \in \mathbf{R}} \varphi(r)| = 3$ , partition according to Algorithm 1:

---

**Algorithm 1** Partition for Case 2.3
 

---

```

1: procedure PARTITION( $N, \mathcal{A}, T, \mathbf{R}$ )
2:    $C_{R_1}; C_{R_2} \leftarrow \{0\}^{N|\mathcal{A}|T}$  ▷ Initialize two sets of counters
3:    $\mathbf{R}_1; \mathbf{R}_2 \leftarrow \emptyset$ 
4:   for element  $e \in \{a, b, c\}$  do
5:      $\mathbf{R}_e \leftarrow \{r | \varphi(r) = e\}$  ▷ Use  $\varphi$  to partition the rows of  $\mathbf{R}$  by constraint type
6:     for  $r \in \mathbf{R}_a$  do
7:        $\mathbf{R}_1 \leftarrow \mathbf{R}_1 \cup r$  ▷ Let  $r \in \mathbf{R}_1$ 
8:       for  $i \in 0 : N|\mathcal{A}|T$  do
9:         if  $r[i] > 0$  then ▷ For each non-zero entry  $\in r$ 
10:           $C_{R_1}[i] \leftarrow C_{R_1}[i] + 1$  ▷ Increment corresponding  $C_{R_1}$  counter
11:       for  $r \in \mathbf{R}_b$  do
12:         flag  $\leftarrow$  false
13:         for  $i \in 0 : N|\mathcal{A}|T$  do
14:           if  $r[i] > 0 \wedge C_{R_1}[i] > 0$  then ▷ If any non-zero element  $r_i$  has  $C_{R_1} > 0$ 
15:             flag  $\leftarrow$  true ▷ Set flag to true
16:         if flag then
17:            $\mathbf{R}_2 \leftarrow \mathbf{R}_2 \cup r$  ▷ Let  $r \in \mathbf{R}_2$ 
18:           for  $i \in 0 : N|\mathcal{A}|T$  do
19:             if  $r[i] > 0$  then ▷ For each non-zero entry  $\in r$ 
20:                $C_{R_2}[i] \leftarrow C_{R_2}[i] + 1$  ▷ Increment corresponding  $C_{R_2}$  counter
21:         else
22:            $\mathbf{R}_1 \leftarrow \mathbf{R}_1 \cup r$  ▷ Let  $r \in \mathbf{R}_1$ 
23:           for  $i \in 0 : N|\mathcal{A}|T$  do
24:             if  $r[i] > 0$  then ▷ For each non-zero entry  $\in r$ 
25:                $C_{R_1}[i] \leftarrow C_{R_1}[i] + 1$  ▷ Increment corresponding  $C_{R_1}$  counter
26:       for  $r \in \mathbf{R}_c$  do
27:          $\mathbf{R}_2 \leftarrow \mathbf{R}_2 \cup r$  ▷ Let  $r \in \mathbf{R}_2$ 
28:         for  $i \in 0 : N|\mathcal{A}|T$  do
29:           if  $r[i] > 0$  then ▷ For each non-zero entry  $\in r$ 
30:              $C_{R_2}[i] \leftarrow C_{R_2}[i] + 1$  ▷ Increment corresponding  $C_{R_2}$  counter
return  $\mathbf{R}_1; \mathbf{R}_2$ 
    
```

---

Taking the column-wise sums of the resulting  $\mathbf{R}_1$  and  $\mathbf{R}_2$  will yield two vectors  $\vec{v}_1, \vec{v}_2 \in \mathbb{Z}^{N|\mathcal{A}|T}$ , which can contain entries  $\in \{0, 1\}$  and  $\{0, 1, 2\}$ , respectively. Note that since  $\vec{v}_2$  is constructed by taking only rows with constraint types  $\in \{b, c\}$ , only entries corresponding to active action columns can take values  $> 1$ . Moreover,  $\forall j \in [N|\mathcal{A}|T], \sum_{i \in \mathbf{R}_2} \mathbf{A}_{ij} = 2 \rightarrow \sum_{i \in \mathbf{R}_1} \mathbf{A}_{ij} = 1$ . Thus,  $\forall j \in [N|\mathcal{A}|T]$ ,

$$\sum_{i \in \mathbf{R}_1} \mathbf{A}_{ij} - \sum_{i \in \mathbf{R}_2} \mathbf{A}_{ij} = 0 - 0 \vee 0 - 1 \vee 1 - 0 \vee 1 - 1 \vee 1 - 2; \{-1, 0, 1\} \subseteq \{-1, 0, 1\} \blacksquare$$

**Case 3**  $R \subseteq A$ . Since  $|\cup_{r \in \mathbf{R}} \varphi(r)| = 3$ , proceed as outlined in Case 2.3. Only a slight modification is required: since  $\mathbf{R}$  is now equal to  $\mathbf{A}$ , taking the column-wise sums of the resulting  $\mathbf{R}_1$  and  $\mathbf{R}_2$  will yield two vectors  $\vec{v}_1, \vec{v}_2 \in \mathbb{Z}^{N|\mathcal{A}|T}$ , which can contain entries  $\in \{1\}$  and  $\{0, 2\}$ , respectively. Thus,  $\forall j \in [N|\mathcal{A}|T]$ ,

$$\sum_{i \in \mathbf{R}_1} \mathbf{A}_{ij} - \sum_{i \in \mathbf{R}_2} \mathbf{A}_{ij} = 1 - 0 \vee 1 - 2; \{-1, 1\} \subsetneq \{-1, 0, 1\} \blacksquare$$

### A.3 Probabilistically Fair Stationary Policy

#### A.3.1 Proof of the Structural Result for Problem (P2) from Section 5.2

Recall that our claimed structural result is: (P2) has an optimal solution in which  $p_i \in (\ell, u)$  for at most one  $i \in B$ , which we now prove.

**PROOF** Note by compactness that (P2) has not just a supremum, but an actual maximum solution. Suppose for contradiction there is some optimal solution  $\vec{p}$  with distinct indices  $i, j \in B$  such that  $p_i, p_j \in (\ell, u)$ . Now, suppose we perturb by an infinitesimal  $\epsilon$  (of arbitrary sign but tiny positive absolute value) such that  $p_i := p_i + \epsilon$  and  $p_j := p_j - \epsilon$ . This satisfies all our constraints for small-enough  $|\epsilon|$ . The change in the objective  $\sum_{i \in B} f_i(p_i)$  is now  $\epsilon \cdot (f'_i(p_i) - f'_j(p_j)) + O(\epsilon^2)$ ; hence, if  $f'_i(p_i) - f'_j(p_j)$  is nonzero, then we can take a tiny  $\epsilon$  of the appropriate sign to increase the objective, a contradiction. Therefore,  $f'_i(p_i) - f'_j(p_j) = 0$ , and so, we now focus on lower-order terms: the change in the objective  $\sum_{i \in B} f_i(p_i)$  is now  $(\epsilon^2/2) \cdot (f''_i(p_i) + f''_j(p_j)) + O(\epsilon^3)$ . However, since  $f_i$  and  $f_j$  are strictly convex, we have that  $f''_i(p_i) + f''_j(p_j) > 0$ , and hence the objective increases regardless of the sign of (the tiny)  $\epsilon$ , again a contradiction. Thus we have our structural result.  $\blacksquare$

#### A.3.2 Probabilistic Fair Stationary Policy Pseudocode

Here we provide pseudocode for the sampling algorithm introduced in Section 5.3, along with its associated SIMPLIFY subroutine [Srinivasan, 2001].

---

**Algorithm 2** Sampling Subroutine (adapted from Srinivasan [2001])

---

```

1: procedure SIMPLIFY( $\alpha \in [0, 1], \beta \in [0, 1]$ )
2:   if  $\alpha = \beta = 0$  then
3:      $p_i, p_j \leftarrow [0, 0]$ 
4:   else if  $\alpha = \beta = 1$  then
5:      $p_i, p_j \leftarrow [1, 1]$ 
6:   else if  $\alpha + \beta = 1$  then
7:     flag  $\leftarrow X \sim B(n = 1, p = \alpha)$ 
8:      $p_i, p_j \leftarrow [1, 0]$  if flag else  $[0, 1]$ 
9:   else if  $0 < \alpha + \beta < 1$  then
10:    flag  $\leftarrow X \sim B(n = 1, p = \frac{\alpha}{\alpha + \beta})$ 
11:     $p_i, p_j \leftarrow [\alpha + \beta, 0]$  if flag else  $[0, \alpha + \beta]$ 
12:   else if  $1 < \alpha + \beta < 2$  then
13:    flag  $\leftarrow X \sim B(n = 1, p = \frac{1 - \beta}{2 - \alpha - \beta})$ 
14:     $p_i, p_j \leftarrow [1, \alpha + \beta - 1]$  if flag else  $[\alpha + \beta - 1, 1]$ 
return  $p_i, p_j$ 

```

---

**Algorithm 3** Sampling Algorithm (adapted from Srinivasan [2001])

---

```

1: procedure SAMPLE( $G = (V, E)$ )
2:    $H \leftarrow G \setminus \{v \mid \exists e \in G \text{ s.t. } e_{\text{dst}} = v\}$ 
3:   if  $|H| = 1$  then return  $G$ 
4:   else if  $|H| \geq 2$  then
5:      $A \subsetneq G \in \binom{H}{\lfloor \frac{|H|}{2} \rfloor}$ 
6:      $B \leftarrow G \setminus A$ 
7:     pairs  $\leftarrow \{(a_i, b_i) \in A \times B \mid i \in \mathcal{I}\}$ 
8:      $H' \leftarrow (V = \emptyset, E = \emptyset)$ 
9:     for  $(v_i, v_j) \in \text{pairs}$  do
10:       $H' \leftarrow H' \cup \{v_i, v_j\}$ 
11:       $H' \leftarrow H' \cup \{v' \mid e_{v', v_\alpha} \mid \alpha \in \{i, j\}\}$ 
12:       $X_i, X_j \leftarrow \text{SIMPLIFY}(p_{v_i}, p_{v_j})$ 
13:       $z_{v_i} \leftarrow X_i$ 
14:       $z_{v_j} \leftarrow X_j$ 
15:      if  $z_{v_i} \in \{0, 1\}$  then
16:         $p_{v'} \leftarrow X_j$ 
17:      else  $p_{v'} \leftarrow X_i$ 
18:    $F \leftarrow G \cup H'$ 
19:   return SAMPLE( $F$ )
    
```

---

$\triangleright$  Select subgraph containing nodes without a parent  
 $\triangleright z_v \in \{0, 1\} \forall v \in G; \sum_v z_v = k$

$\triangleright$  Defined in Algorithm 2  
 $\triangleright$  If  $X_i$  was fixed,  $z_{v_i} \in \{0, 1\}$   
 $\triangleright$  If  $X_j$  was fixed,  $z_{v_j} \in \{0, 1\}$

$\triangleright \forall v \in G \cap H'$ , update attribute values per  $H'$

---

#### A.4 Heuristics

In Section 6, three heuristics based on the THRESHOLD WHITTLE algorithm are introduced: FIRST, LAST, and RANDOM. Here, we go into more detail and provide pseudocode.

**Definition A.1** *Within the context of Algorithm 4, we define a constrained pull to be one that is executed to satisfy a hard integer periodicity constraint. Only arms that have not yet been pulled the required number of times within the  $\nu$ -length interval are available; other arms are excluded from consideration, unless all arms have already satisfied their constraints. In this case, all arms are available to be pulled.*

If a pull is not constrained, we say it is *unconstrained* or *residual*.

The FIRST heuristic requires that all constrained pulls must occur at the start of the interval. This implies that the first  $N/k$  timesteps in each interval are dedicated to pulling all  $N$  arms.

The LAST heuristic requires that all constrained pulls must occur at the end of the interval. Unlike the FIRST heuristic, not all arms will necessarily be pulled in the last  $N/k$  timesteps, as some arms will have already satisfied their constraint earlier in the interval on the unconstrained pulls. These leftover constrained pulls function as unconstrained pulls, per Definition A.1.

The RANDOM heuristic chooses random positions within the interval for constrained pulls to occur. Similarly to the LAST heuristic, some of the later constrained pulls may become unconstrained pulls if all arms have already satisfied their constraint earlier in the interval.

---

#### Algorithm 4 Periodicity Constraint-Enforcing Heuristic Based on THRESHOLD WHITTLE

---

```

1: procedure SIMULATION( $A, T, \nu, k$ )
2:   for interval  $\in [0, T]$  with step size  $\nu$  do
3:      $C_{\text{interval}} \leftarrow \emptyset$  ▷  $C_{\text{interval}} := \text{arm(s) with constraint satisfied during the interval}$ 
4:
5:     for  $a \in A$  do
6:        $a.\text{last observed state} \leftarrow 1$ 
7:        $a.\text{time since pull} \leftarrow 1$ 
8:
9:     for  $t \in T$  do
10:       $i \leftarrow \text{GetInterval}(t)$ 
11:
12:      if  $t$  is a constrained pull  $\wedge C_i \subsetneq A$  then ▷ Consider arms with constraint not yet satisfied in interval
13:         $A' \leftarrow \{a | a \in A \setminus C_i\}$ 
14:      else if  $t$  is a residual pull  $\vee C_i = A$  then ▷ Consider all arms
15:         $A' \leftarrow A$ 
16:
17:       $A'_k \leftarrow \text{SelectTopK}(A', k, t)$  ▷ Select  $k$  arms with highest Whittle index
18:       $C_i \leftarrow C_i \cup A'_k$ 
19:
20:      for  $a \in A$  do
21:         $s_{t+1}(a) \leftarrow \text{UpdateState}(a)$  ▷ Update each arm's state using belief
    return

```

---

#### A.5 Additional Experimental Results

In this section, we present additional experimental results. Appendix A.5.1 discusses the distribution of actions in THRESHOLD WHITTLE, Appendix A.5.2 discusses the true optimal policy (found using the IP presented in Appendix A.2), and Appendices A.5.3 & A.5.4 give additional results for the experiments presented in Sections 6.1 & 6.2, respectively. Code and instructions needed to reproduce these experimental results are included in the supplemental material.

We have run simulations on an Intel(R) Core i7 CPU with 16Gb of RAM. Results and logs for the experiments described below require approximately 25Gb of disk space. Simulations are configurable via configuration files; runs are trivially parallelizable via these configuration files. For parallelization, we ran these experiments on a cluster of computational (CPU) resources with 192 cores and 3.4TB of memory available over 8 nodes. All of these compute

nodes are networked with 25Gb Ethernet networking and have access to 152TB of scale out network attached storage. However, the computational needs of our code are relatively minor.

### A.5.1 Inequity in the Distribution of Action Allocation in Whittle Index Policies

Here, we present numerical results confirming Prins et al. [2020]’s findings that THRESHOLD WHITTLE tends to allocate pulls according to a bimodal distribution: a subset of arms are pulled frequently, while others are largely ignored.

**Experimental Setup.** For each iteration, we generate  $N = 2$  forward threshold optimal arms and run THRESHOLD WHITTLE for a  $T = 365$  horizon simulation, where the budget constraint  $k = 1$ . We run 1,000 such iterations.

**Results.** The arms’ Whittle indices in 515 out of 1,000 simulations (51.5%) never overlap, meaning for *any* combination of initial states, state transitions, and pulls, THRESHOLD WHITTLE would pull one arm for all timesteps  $t \in T$  and completely ignore the second arm.

We visualize one such case in Figure 6. Recall that THRESHOLD WHITTLE precomputes one subsidy  $m$  per arm and belief combination. Since belief is a function of last known state  $s \in \{0, 1\}$  and time-since-seen  $u \in [T]$  (using the notation of Mate et al. [2020]), we plot the subsidy of each arm and state with time-since-seen  $u$  on the  $x$ -axis. There exists a horizontal line that divides the two arms, so arm  $i = 1$  will be pulled for every timestep  $t \in T$  and arm  $i = 2$  will never be pulled.

In Section 4.1, we discuss plausible modifications to  $m$ . These modifications would need to ensure that no such horizontal line exists; indeed, the lines associated with the arms in Figure 6 must cross before  $\nu$  timesteps elapse to guarantee hard integer periodicity constraint satisfaction.

Another perspective we can take is to ask: what’s the smallest interval  $\nu_i$  for each arm  $i$  we could have specified such that THRESHOLD WHITTLE would have satisfied the hard integer periodicity constraint? Note that this is retrospective—there is no way to enforce this constraint at the outset.

We visualize the minimum such  $\nu_i$  in Figure 7. On the far right, we see the 515 cases where (without loss of generality) the second arm is never pulled, that is, the minimum  $\nu_i$  such that THRESHOLD WHITTLE satisfies the hard integer periodicity constraint must be *larger* than the horizon,  $T = 365$ . There is one case where arm  $i = 2$  was pulled exactly once; THRESHOLD WHITTLE pulls each arm far more frequently in the remaining 484 simulations, as shown on the left of Figure 7.

### A.5.2 Comparison with the True Optimal Policy

In Section 6, we compare intervention benefit against THRESHOLD WHITTLE, which is asymptotically optimal for forward threshold optimal transition matrices under a budget constraint  $k$  [Mate et al., 2020]. However, with the integer program (IP) we formulate in Appendix A.2, we can find the optimal policy for any set of transition matrices under budget *and* fairness constraints as long as  $N$  and  $T$  are small.

We generate  $N = 2$  random arms such that the structural constraints outlined in Section 2.1 are satisfied. We set  $k = 1$  and  $T = 6$ . Though the variance in reward is large due to

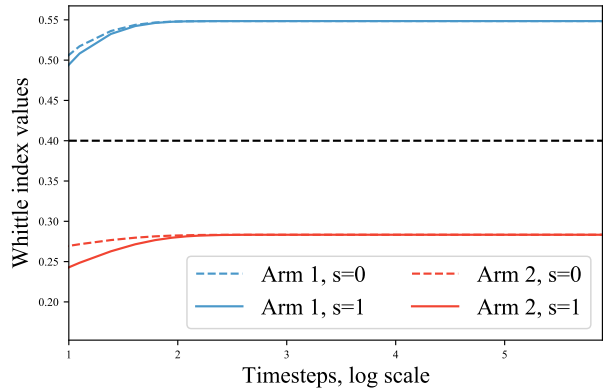


Figure 6: Whittle index subsidies, TW

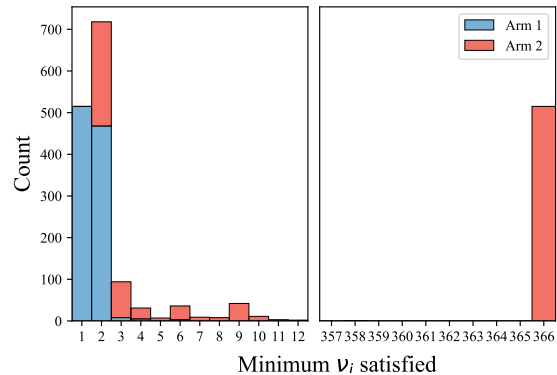


Figure 7: Minimum  $\nu_i$ , THRESHOLD WHITTLE

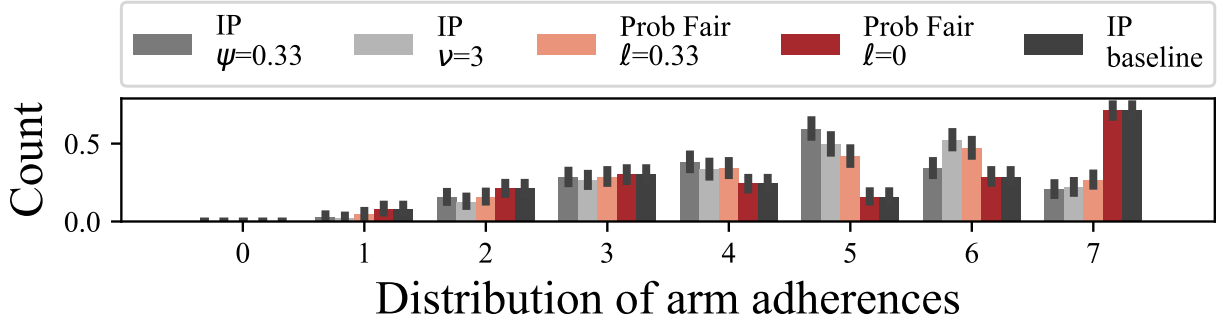


Figure 8: Adherences, compared to the IP formulation

the small  $T$ , Figure 8 shows that PROBFair obtains 100% of the intervention benefit when no fairness constraints are applied. Similarly, PROBFair with  $\ell = 0.33$  obtains the same adherence behavior as the IP policy with under hard fairness constraint  $\nu = 3$  or minimum selection fraction constraint  $\psi = 0.33$ . (within 95% confidence interval shown). All results shown are bootstrapped over 500 iterations.

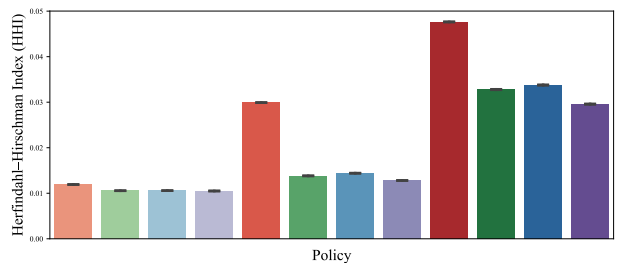
**Minimum Selection Fraction Constraints.** As we discuss in Appendix A.5.1, the optimal policy is often to pull the same  $k$  arms at every timestep and ignore all other arms. Under minimum selection fraction constraints, each arm must be pulled at least a minimum fraction  $\psi$  of  $T$  rounds, with no conditions on when these pulls should take place. We confirm with the truly optimal IP implementation our intuition that these additional pulls are allocated at the beginning or end of the simulation. That is, the optimal policy under minimum selection fraction constraints is to take advantage of the finite time horizon, which is not suitable for the applications we consider.

### A.5.3 Additional CPAP Simulation Results

To augment the results in Section 6.1, we present additional distributional results as well as results for  $\alpha_{\text{intrv}} = 1.2$  and  $T = 30$ . For all plots in this section and the following, we use the legend in Figure 9.

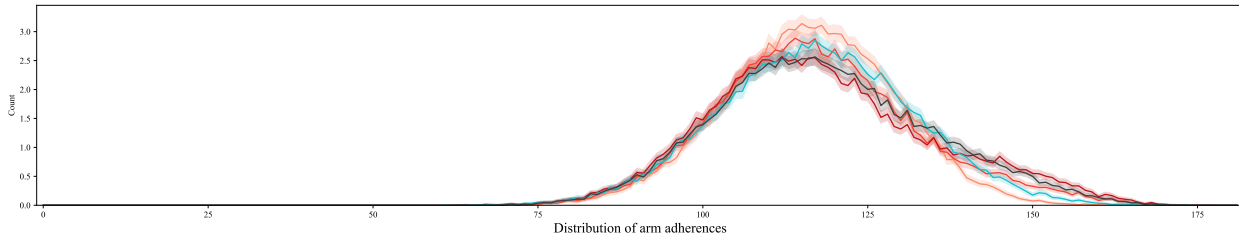
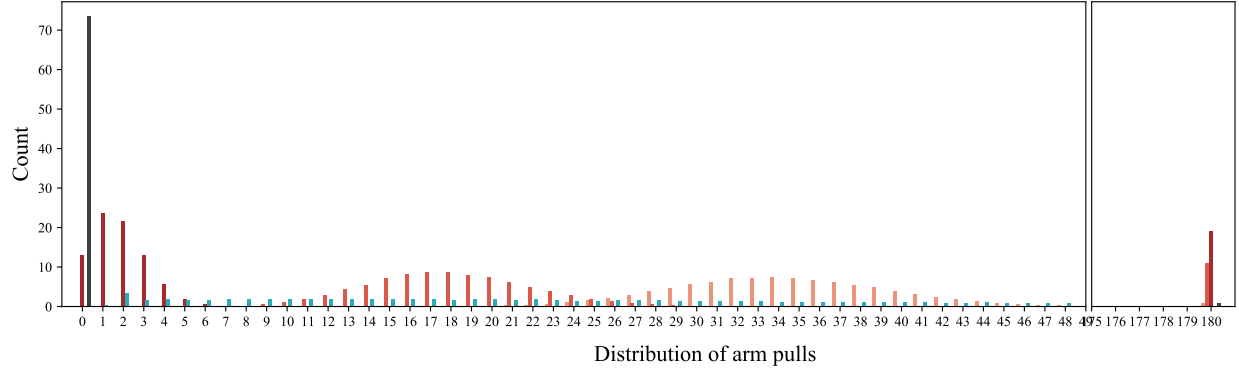
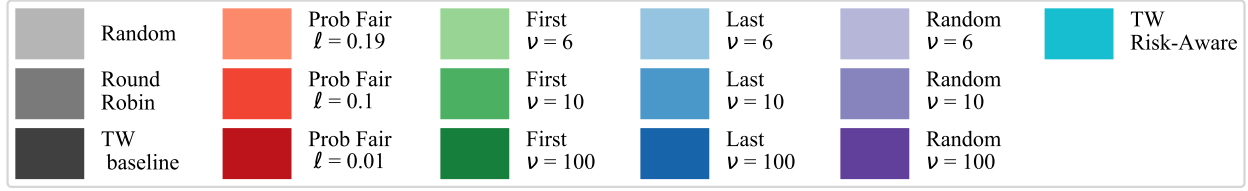
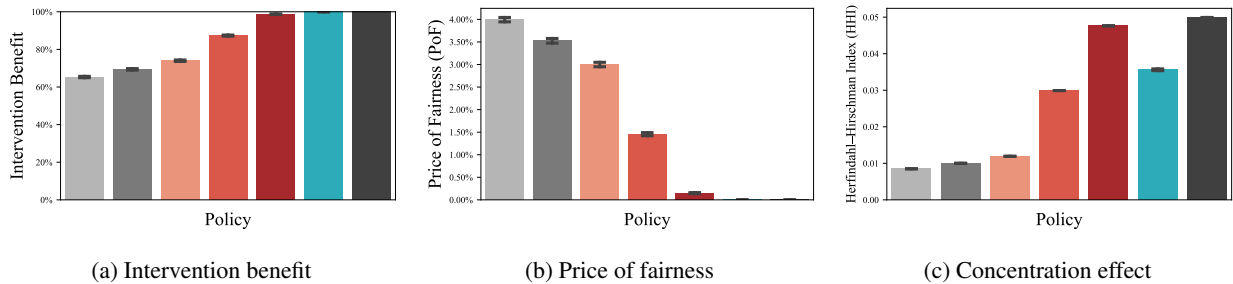
**Additional results for  $\alpha_{\text{intrv}} = 1.1$  and  $T = 180$ .** In Figure 9, we present the distribution of actions and adherences resulting from PROBFair, RISK-AWARE WHITTLE, and THRESHOLD WHITTLE. Just like in Figure 7, THRESHOLD WHITTLE pulls the same  $k$  arms at each timestep and otherwise ignores arms (as indicated by the spikes on the right and left of Fig. 9a, respectively). The fairness-incentivizing algorithms PROBFair and RISK-AWARE WHITTLE shift this distribution with little change in overall adherence (as shown in Fig. 9b). This is a highly adherent group—arms adhere at least 50% of the time in general—but even under THRESHOLD WHITTLE no patient arm has perfect adherence in the simulation.

Though our algorithm obtains a better intervention benefit than RISK-AWARE WHITTLE for these parameters (Fig. 2), it has higher concentration effect versus the heuristics (Fig. 10).


 Figure 10: Concentration effect versus heuristics,  $\alpha_{\text{intrv}} = 1.1$  and  $T = 180$ , on the CPAP dataset

**Larger Intervention Effect.** Figure 11 shows results for a larger intervention effect,  $\alpha_{\text{intrv}} = 1.2$ . Here, PROBFair with  $\ell = 0.01$  obtains nearly the same intervention benefit as THRESHOLD WHITTLE (Fig. 11a) and so its price of fairness is very small (Fig. 11b), however, the concentration effect corresponding to this  $\ell$  is higher than RISK-AWARE WHITTLE (Fig. 11c).

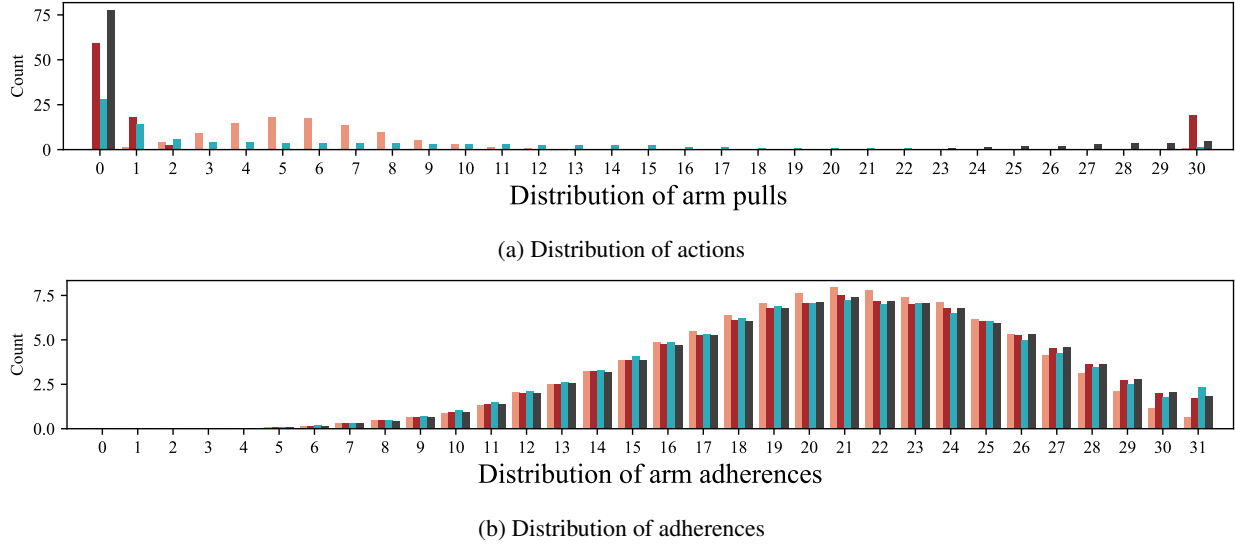
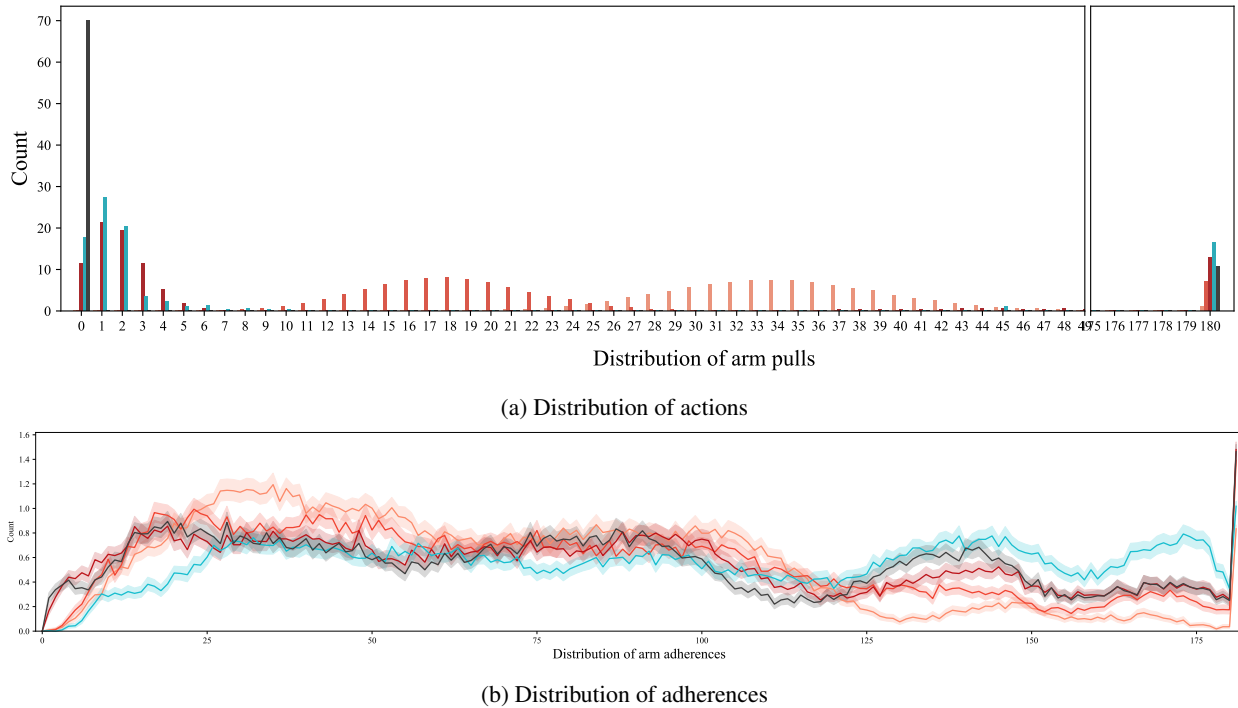
**Smaller Horizon.** Since program lengths may be quite short, we provide results for the smaller horizon  $T = 30$ . The distributions shown in Figure 12 are miniaturized versions of the same plots for  $T = 180$  in Figure 9, indicating that convergent behavior occurs quickly (as we would expect).


 Figure 9: Additional results for  $\alpha_{\text{intrv}} = 1.1$  and  $T = 180$ , on the CPAP dataset

 Figure 11:  $\alpha_{\text{intrv}} = 1.2$  and  $T = 180$ , on the CPAP dataset.

#### A.5.4 Additional Synthetic Data Results

In Section 6.2, we present results for a random transition matrix cohort. Here, we present additional results, as well as results on forward, reverse, and mixed cohorts below. It is clear from these results that while PROBFair guarantees fairness with a configurable value  $\ell$ , its relative intervention benefit, price of fairness, and concentration effect versus Whittle-based algorithms varies.

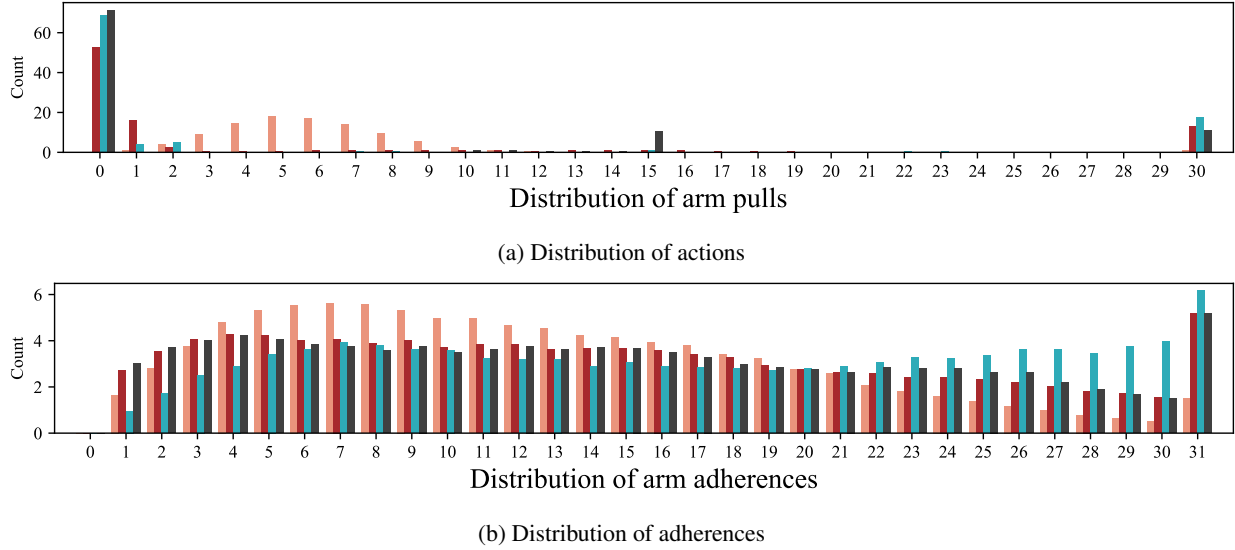
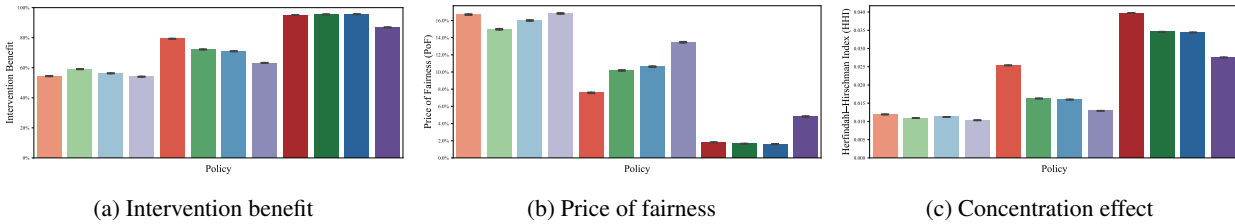
Within the context of this section, we generate forward and reverse threshold optimal arms under the local reward function  $r(b) = b$ . Thus, **THRESHOLD WHITTLE** is the asymptotically optimal policy under forward threshold matrices. The policy **RISK-AWARE WHITTLE**, with  $r(b) = -e^{\lambda(1-b)}$ , may not be asymptotically optimal for these transition matrix cohorts. However, by the conditions for forward (reverse) threshold optimality given in Theorem 1 (2) of Mate et al. [2021], all transition matrices are reverse threshold optimal for that policy. (**THRESHOLD WHITTLE** and


 Figure 12:  $\alpha_{\text{intrv}} = 1.1$  and  $T = 180$ , on the CPAP dataset

 Figure 13: Additional results for  $N = 100$  randomly generated arms,  $T = 180$ 

its risk-aware variants have been proven asymptotically optimal for only forward threshold optimal transition matrices, but experimental results are promising for other transition matrix types [Mate et al., 2020].)

**Random Cohort.** Figure 13 gives the action and adherence distributions associated with the results shown in Figure 3. Though it is not shown, THRESHOLD WHITTLE pulls  $\approx 10\%$  of arms at 90, i.e. 50% of the time (in Fig. 14a, the analogous  $T = 30$  plot, this dramatic increase in pulls is visible). Both fairness inducing algorithms (RISK-AWARE WHITTLE and PROBFAR) reduce the number of neglected arms as expected. Interestingly, RISK-AWARE WHITTLE and PROBFAR with  $\ell = 0.01$  pull more arms at every timestep than THRESHOLD WHITTLE.




 Figure 14: Additional results for  $N = 100$  randomly generated arms,  $T = 30$ 

 Figure 15: Heuristics comparison results for  $N = 100$  randomly generated arms,  $T = 180$ 

The impact of these actions on adherence patterns are shown in Figure 13b. Since these arms are randomly generated, we expect the underlying distribution of adherence to look more uniform and have larger variance than e.g., the CPAP dataset (Fig. 9b). All of the algorithms shown have a dramatic increase in the number of arms that are adherent for all timesteps, however, this number for RISK-AWARE WHITTLE is half that of THRESHOLD WHITTLE. This is perhaps why there are more arms that are adherent most of the time under RISK-AWARE WHITTLE as opposed to the other algorithms, and augments our point in Section 6.2 that THRESHOLD WHITTLE is a preferable choice over RISK-AWARE WHITTLE for this cohort.

Just like in the CPAP simulations (Fig. 12), these results are the same for smaller program horizons, allaying any concerns about convergence for short programs (Fig. 14).

Finally, we give comparisons on the random cohort against the three heuristics options in Figure 15. Though PROBFair generates larger intervention benefit and therefore smaller price of fairness overall, the concentration effect of our algorithm is larger than that of the heuristics. The relative values shown here are largely consistent with the other cohort types we simulate (see Figs. 16, 17, & 19).

**Forward Threshold Optimal Cohort.** As we note above, THRESHOLD WHITTLE is guaranteed to be asymptotically optimal for forward threshold optimal transition matrices, and, as we see in Figure 16, RISK-AWARE WHITTLE obtains 100% intervention benefit as well. However, the concentration effect of RISK-AWARE WHITTLE is substantially higher than THRESHOLD WHITTLE. PROBFair provides a nice alternative to either policy with good intervention benefit and concentration effect results (and, of course, probabilistic fairness guarantees).

**Reverse Threshold Optimal Cohort.** The results for the reverse threshold optimal cohort are unusual, perhaps because the Whittle-based algorithms are developed for *forward* threshold optimal arms. Though the distribution of arm allocations mirrors that for other cohorts (Fig. 18a), the rewards are larger. Figure 17a shows the intervention benefit of the algorithms; oddly, RISK-AWARE WHITTLE obtains triple the reward of THRESHOLD WHITTLE, so its intervention

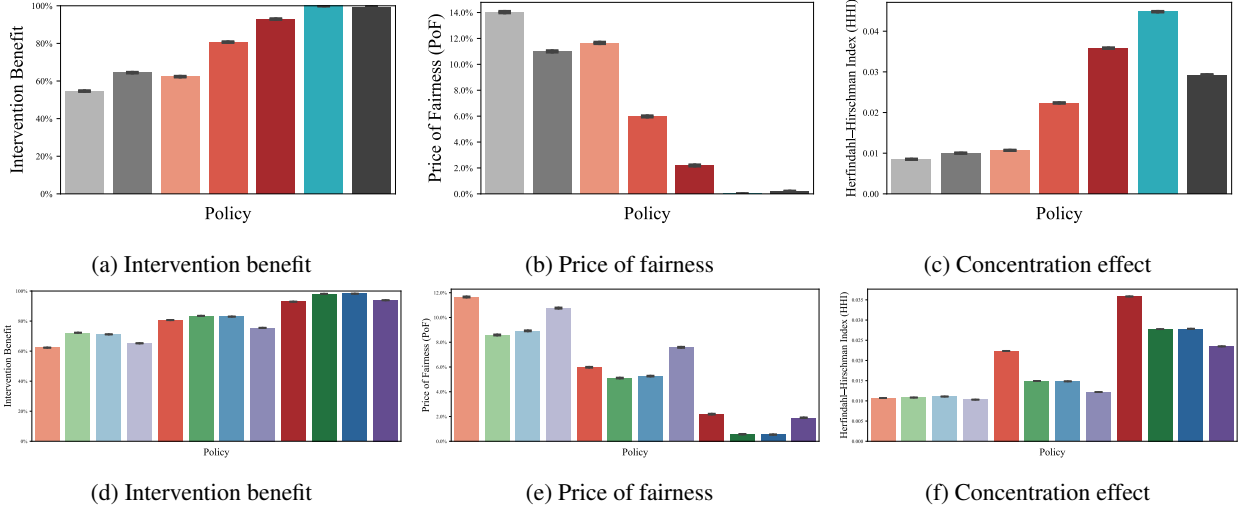


Figure 16: Results for  $N = 100$  forward threshold optimal arms,  $T = 180$

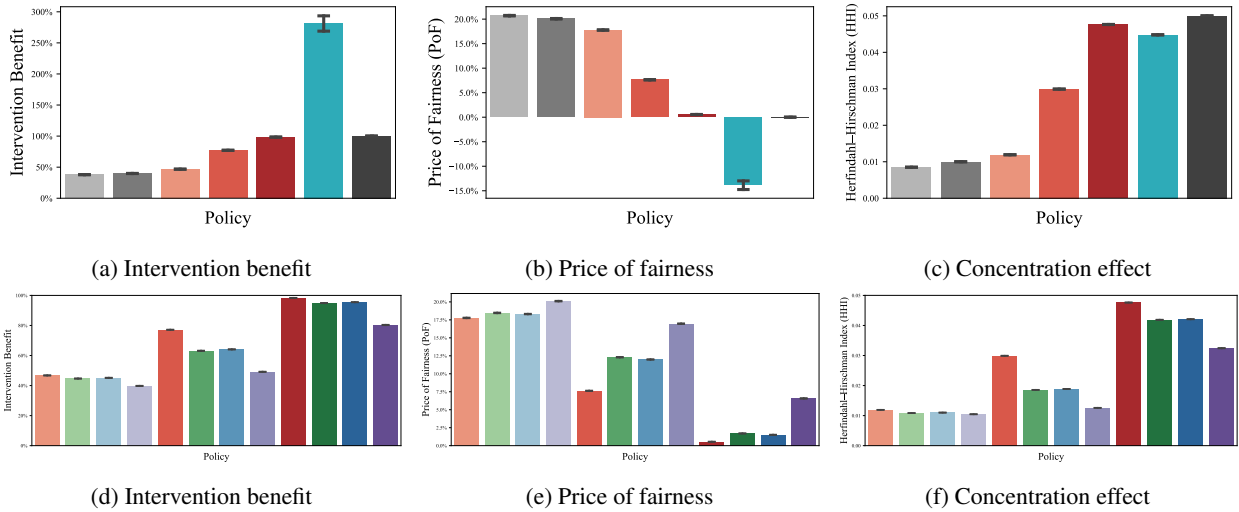


Figure 17: Results for  $N = 100$  reverse threshold optimal arms,  $T = 180$

benefit is larger than 100%. This explains the negative price of fairness of RISK-AWARE WHITTLE (recall that price of fairness is normalized by THRESHOLD WHITTLE).

**Mixed Forward and Reverse Threshold Optimal Cohort.** Finally, we consider a mixed cohort of 50 forward and 50 reverse threshold optimal arms in Figure 19. Unlike for the reverse cohort, RISK-AWARE WHITTLE obtains 100% of the intervention benefit of THRESHOLD WHITTLE (Fig. 19a). PROBFAIR obtains similar results as previous cohorts—competitive intervention benefit, price of fairness, and concentration effects while guaranteeing probabilistic fairness.

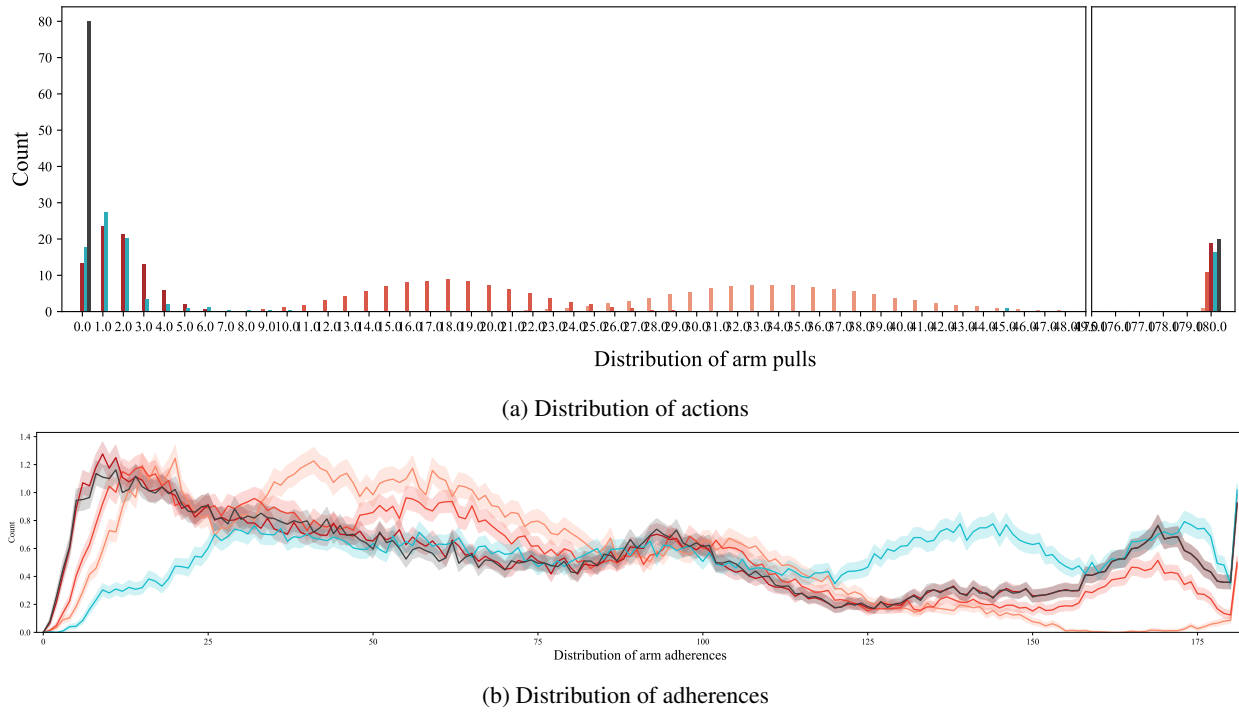


Figure 18: Additional results for  $N = 100$  reverse threshold optimal arms,  $T = 180$

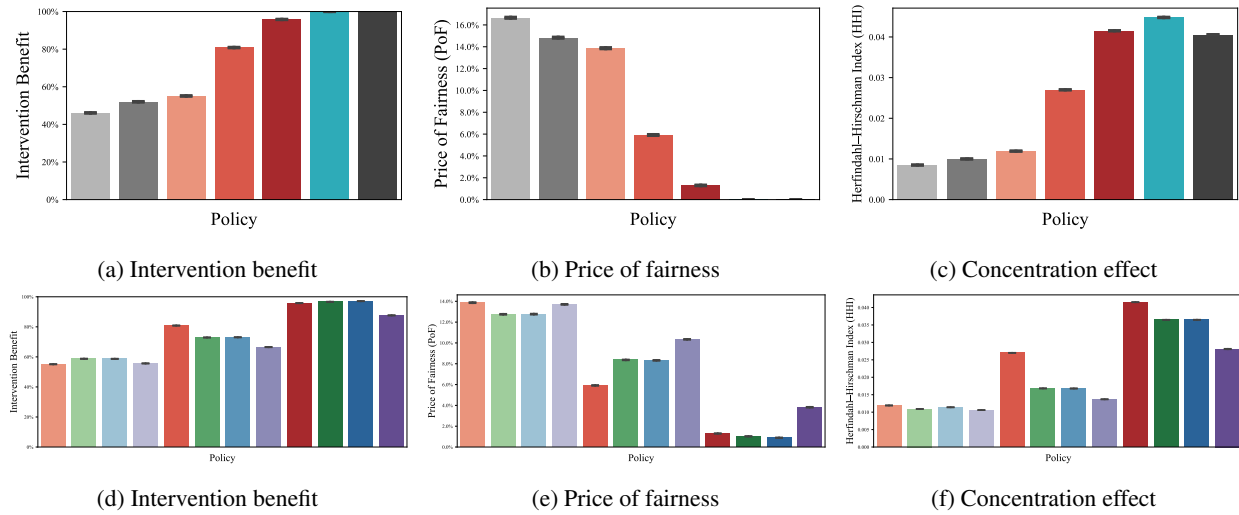


Figure 19: Results for a mixed cohort of 50 forward and 50 reverse threshold optimal arms,  $T = 180$